

Mechanism for the suppression of quantum noise at large scales on expanding space

Samuel Colin, Antony Valentini
*Department of Physics and Astronomy,
Clemson University, 303 Kinard Laboratory,
Clemson, SC 29634-0978, USA.*

We present an exactly-solvable model for the suppression of quantum noise at large scales on expanding space. The suppression arises naturally in the de Broglie-Bohm pilot-wave formulation of quantum theory, according to which the Born probability rule has a dynamical origin. For a scalar field on a radiation-dominated background we construct the exact solution for the time-evolving wave functional and study properties of the associated field trajectories. It is shown that the time evolution of a field mode on expanding space is mathematically equivalent to that of a standard harmonic oscillator with a ‘retarded time’ that depends on the wavelength of the mode. In the far super-Hubble regime the equivalent oscillator evolves over only one Hubble time, yielding a simple mechanism whereby relaxation to the Born rule can be suppressed on very large scales. We present numerical simulations illustrating how the expansion of space can cause a retardation of relaxation in the super-Hubble regime. Given these results it is natural to expect a suppression of quantum noise at super-Hubble wavelengths. Such suppression could have taken place in a pre-inflationary era, resulting in a large-scale power deficit in the cosmic microwave background.

1 Introduction

According to inflationary cosmology [1, 2, 3, 4], the temperature anisotropy that is observed in the cosmic microwave background (CMB) was ultimately seeded by quantum fluctuations at very early times. During inflation the universe undergoes a period of exponential expansion with a scale factor $a(t) \propto e^{Ht}$ (with $H \approx \text{const.}$). The expansion is driven by the energy density of an approximately-homogeneous scalar field, whose spatially homogeneous and inhomogeneous parts we respectively denote ϕ_0 and ϕ . The anisotropy in the CMB was generated by primordial curvature perturbations $\mathcal{R}_{\mathbf{k}}$ that in turn were generated by quantum fluctuations of ϕ in the Bunch-Davies vacuum. Measurements of the CMB spectrum may therefore be used to probe the early quantum vacuum. For this reason inflation has long been regarded as a testing ground for high-energy physics – for example to probe possible high-frequency corrections to the inflationary vacuum state [5, 6, 7, 8, 9, 10, 11, 12, 13, 14].

Because the primordial perturbations have a quantum origin, inflation may equally be used to test quantum theory itself (at very short distances and at very early times). Several authors have discussed how inflationary CMB predictions would be affected by a hypothetical dynamical collapse of the wave function in the early universe (introduced in order to solve the quantum measurement problem) [15, 16, 17]. Another line of enquiry considers the possibility of ‘quantum nonequilibrium’ in the inflationary vacuum [18, 19, 20], which can arise in the de Broglie-Bohm pilot-wave formulation of quantum theory [21, 22, 23, 24, 25]. Quantum nonequilibrium generates corrections to quantum probabilities without affecting the quantum state, and therefore changes the spectrum of the vacuum fluctuations without changing the vacuum wave functional itself. Measurements of the CMB may then be used to test for the existence of quantum nonequilibrium at very early times [20].

In pilot-wave theory, a system with configuration q has a wave function $\psi(q, t)$ obeying the usual Schrödinger equation $i\partial\psi/\partial t = \hat{H}\psi$ (we take $\hbar = 1$). In addition, the system has an actual configuration $q(t)$ evolving in time with a velocity $\dot{q} \equiv dq/dt$ that is determined by ψ .¹ For systems with standard Hamiltonians, \dot{q} is proportional to the gradient $\partial_q S$ of the phase S of ψ . More generally, $\dot{q} = j/|\psi|^2$ where $j = j[\psi] = j(q, t)$ is the current associated with the Schrödinger equation [26].² The current satisfies a continuity equation

$$\frac{\partial |\psi|^2}{\partial t} + \partial_q \cdot j = 0 . \tag{1}$$

For an ensemble of systems with initial wave function $\psi(q, t_i)$, we may in prin-

¹Note the distinction between a general point q in configuration space and the actual point $q(t)$ occupied by the system at time t .

²At the fundamental level ψ has no *a priori* connection with probabilities; instead ψ plays the role of a ‘pilot wave’ in configuration space that guides the motion of an individual system. Because ψ is a field in configuration space and not an ordinary field in 3-space, it does not itself carry energy or momentum. For a detailed discussion of the interpretation of this theory see ref. [27]. Historically, the theory was first proposed by de Broglie at the 1927 Solvay conference [22].

ple consider an arbitrary initial distribution $\rho(q, t_i)$ of configurations $q(t_i)$. Because each system has velocity \dot{q} , the time evolution $\rho(q, t)$ of the distribution is determined by the continuity equation

$$\frac{\partial \rho}{\partial t} + \partial_q \cdot (\rho \dot{q}) = 0 . \quad (2)$$

Since $|\psi|^2$ obeys the same equation, an initial distribution $\rho(q, t_i) = |\psi(q, t_i)|^2$ evolves into $\rho(q, t) = |\psi(q, t)|^2$. This is the state of ‘quantum equilibrium’, for which the distribution matches the Born probability rule. But the dynamics also allows us to consider ‘nonequilibrium’ distributions $\rho(q, t_i) \neq |\psi(q, t_i)|^2$ [28, 29, 30] – just as classical mechanics allows us to consider initial distributions that depart from thermal equilibrium.

It is well known that the empirical predictions of quantum theory follow from pilot-wave dynamics if it is assumed that the initial ensemble is in quantum equilibrium, with a distribution $\rho(q, t_i) = |\psi(q, t_i)|^2$. This was shown fully by Bohm in 1952 [23, 24]. A key point in the derivation is to apply the dynamics to the measuring apparatus as well as to the microscopic system. The distribution of apparatus readings or outcomes then agrees with quantum theory. However, in general the distribution of outcomes depends on the assumed initial distribution $\rho(q, t_i)$ of configurations. For an initial nonequilibrium ensemble, with $\rho(q, t_i) \neq |\psi(q, t_i)|^2$, the distribution of quantum measurement outcomes will generally disagree with the predictions of quantum theory. Thus, at least in principle, pilot-wave theory contains a physics that is much wider than quantum physics, with possible nonequilibrium distributions that violate the usual Born rule [28, 29, 30, 31, 32, 33, 18, 19, 34, 20, 35]. Such distributions give rise to new phenomena such as nonlocal signalling [29] – acting along an underlying preferred foliation of spacetime [36] – and ‘subquantum’ measurements that violate the uncertainty principle [33, 35]. Quantum physics is then seen as a special equilibrium case of a much wider nonequilibrium physics.

In pilot-wave theory, the equilibrium state $\rho = |\psi|^2$ arises from a process of relaxation that is analogous to classical thermal relaxation. The H -function

$$H = \int dq \rho \ln(\rho / |\psi|^2) \quad (3)$$

(minus the relative entropy of ρ with respect to $|\psi|^2$) quantifies the difference between ρ and $|\psi|^2$. It obeys a coarse-graining H -theorem analogous to the classical one, where the minimum $H = 0$ corresponds to equilibrium [28, 30, 32]. For initial wave functions that are superpositions of different energy eigenfunctions, extensive numerical evidence shows that initial nonequilibrium distributions ρ rapidly approach $|\psi|^2$ on a coarse-grained level (assuming that the initial state has no fine-grained micro-structure) [30, 32, 37, 38, 39, 40], with an approximately exponential decay of the coarse-grained H -function [37, 39]. All the systems that we have experimental access to have had a long and violent astrophysical history. Therefore today we would expect to see quantum equilibrium

for these systems (such as atoms in the laboratory). And indeed experiment has confirmed the Born rule in a wide range of conditions.

On the other hand it is conceivable that quantum nonequilibrium existed in the early universe, at very early times before relaxation took place [28, 29, 30, 31, 32, 18, 19, 34, 20]. This is certainly a possibility, in the sense that pilot-wave theory would allow it. It is also (arguably) to be expected, since an equilibrium state today will naturally have arisen by a process of relaxation from an earlier nonequilibrium state (as in ordinary statistical mechanics). Further motivations may be given for the hypothesis of quantum nonequilibrium in the remote past, including certain otherwise-puzzling ‘conspiratorial’ or ‘finely-tuned’ features of quantum theory, and a possible solution to the early homogeneity problem (which afflicts even some models of inflation) [28, 29, 30, 31, 32, 20].

Quantum nonequilibrium during the inflationary phase could certainly leave an imprint today in the CMB. It was shown in ref. [20] that, if the inflaton field ϕ is in a state of quantum nonequilibrium at the onset of inflation, then the power spectrum for primordial curvature perturbations $\mathcal{R}_{\mathbf{k}}$ will be given by $\mathcal{P}_{\mathcal{R}}(k) = \mathcal{P}_{\mathcal{R}}^{\text{QT}}(k)\xi(k)$, where $\mathcal{P}_{\mathcal{R}}^{\text{QT}}(k)$ is the usual quantum-theoretical prediction and $\xi(k)$ is a ‘nonequilibrium function’ that is equal to the ratio of the nonequilibrium and quantum variances for the Fourier components $\phi_{\mathbf{k}}$. (It was shown that this ratio is preserved in time during the inflationary expansion itself.) Measurements of the angular power spectrum C_l for the CMB may then be used to set empirical bounds on $\xi(k)$ – that is, to set limits on corrections to the Born rule during inflation. The hypothesis of quantum nonequilibrium at or close to the big bang can therefore be tested using inflationary cosmology.

A more ambitious task is to predict some features of the function $\xi(k)$. One possible strategy is to consider a pre-inflationary era and to derive constraints on residual nonequilibrium from that time. It was suggested in ref. [18] that relaxation could be suppressed for super-Hubble field modes in a radiation-dominated universe, opening up the possibility that in some circumstances nonequilibrium would survive until later times. In refs. [19, 41] such suppression is shown to occur by means of an upper bound on the mean displacement of trajectories in configuration space, resulting in a ‘freezing inequality’ that implies relaxation suppression for super-Hubble modes (when the inequality is satisfied). However, the inequality depends on the unknown time evolution of the quantum state and is difficult to evaluate. On this basis it was suggested in refs. [18, 19, 20] that – in a cosmology with a radiation-dominated pre-inflationary phase – there would exist a large-scale power deficit in the CMB, above some comoving wavelength λ_c that remained to be estimated. For several years the existence of an infra-red power deficit in the *WMAP* data was controversial [42], but such a deficit has recently been confirmed in the *Planck* data [43]. The statistical significance is not high: the deficit might be a mere fluctuation. Even so, it is worth exploring physical models that predict such a deficit in order to better assess its nature and significance. Therefore we return to this theme here.

In this paper we present an exactly-solvable model of the suppression of relaxation for super-Hubble modes on expanding space, resulting in a suppression

of quantum noise at large scales. For a free scalar field in a radiation-dominated universe we find the exact solution for the time-evolving wave functional and we demonstrate certain properties of the associated de Broglie-Bohm trajectories. In particular, we show that the time evolution of a field mode on expanding space is mathematically equivalent to the time evolution of a standard harmonic oscillator – but with real time replaced by a ‘retarded time’ that depends on the wavelength of the mode. In the far super-Hubble regime we find that the equivalent oscillator evolves over only one Hubble time. This result yields a simple mechanism whereby relaxation to the Born rule can be suppressed at very large scales. We also provide numerical simulations illustrating how the expansion of space can cause a suppression (or retardation) of relaxation in the super-Hubble regime. These exact results broadly confirm the expected relaxation suppression for super-Hubble modes that was proposed in refs. [18, 19, 20].

In the light of these results, it is natural to expect a suppression of quantum noise at super-Hubble wavelengths in a radiation-dominated expansion (if nonequilibrium existed at the beginning of the expansion). As noted, such suppression could have taken place in a pre-inflationary era, resulting in a power deficit in the inflationary spectrum above some large wavelength λ_c [20]. Here we shall provide a simple estimate of the cutoff λ_c , which is found to depend essentially on the number N of inflationary e-folds and on the reheating temperature T_{end} at the end of inflation. We find that the allowed parameter space for N and T_{end} is consistent with a cutoff λ_c corresponding to the scale of the power deficit observed in the CMB by the *Planck* satellite [43]. It is therefore conceivable that the observed deficit is caused by the mechanism discussed in this paper. It is also quite possible that in the real universe our λ_c is so large as to yield a negligible effect on the CMB – for example, if the number N of e-folds is very large. This remains to be seen. Here we are mostly concerned with demonstrating a general mechanism for quantum noise suppression at large scales. The detailed application of this mechanism to specific cosmological models, and an evaluation of the significance of the results compared with rival models, is left for future work.

It should be emphasised that a suppression of power at large scales arises quite naturally in the de Broglie-Bohm formulation of quantum theory, according to which quantum noise has a dynamical origin. The dynamics itself generates a rapid relaxation in the sub-Hubble regime and a suppression of relaxation in the super-Hubble regime. The value of the comoving lengthscale λ_c above which such suppression occurs will, however, depend on the cosmological model.

Finally, we note that a cosmology with a radiation-dominated pre-inflationary phase has been considered by some authors [44, 45, 46, 47, 48]. (For a discussion of motivations for such a cosmology, see ref. [47].) Working in terms of standard quantum theory, a pre-inflationary era can yield corrections to the inflationary vacuum with a resulting power deficit at large scales [47, 48]. To distinguish the latter effect from that studied here would require detailed predictions for the nonequilibrium function $\xi(k)$ (see Section 8).

In Section 2 we present the pilot-wave dynamics of a scalar field on expanding space. In Section 3 we find the exact solution for the wave function of a

single mode in the case of a radiation-dominated expansion. In Section 4 we discuss the associated de Broglie-Bohm velocity field and we demonstrate that the dynamics is equivalent to that of a standard harmonic oscillator with a retarded time. This result is used in Section 5 to show that quantum nonequilibrium can be frozen in the far super-Hubble regime. In Section 6 we present numerical simulations that illustrate the suppression of quantum noise at super-Hubble wavelengths. In Section 7 we outline a possible application of this mechanism to cosmology. We briefly review how quantum nonequilibrium in the inflationary vacuum can cause a large-scale power deficit in the CMB, and we discuss how such nonequilibrium could arise from a super-Hubble suppression of relaxation during a pre-inflationary phase. Our conclusions and suggestions for future work are given in Section 8.

2 Pilot-wave dynamics of a scalar field on expanding space

A free, minimally-coupled, and massless scalar field ϕ on a curved spacetime with 4-metric $g_{\mu\nu}$ has a classical Lagrangian density

$$\mathcal{L} = \frac{1}{2} \sqrt{-g} g^{\mu\nu} \partial_\mu \phi \partial_\nu \phi . \quad (4)$$

We shall work on an expanding flat space with line element

$$d\tau^2 = dt^2 - a^2 d\mathbf{x}^2 , \quad (5)$$

where $a = a(t)$ is the scale factor and we take $c = 1$. We then have

$$\mathcal{L} = \frac{1}{2} a^3 \dot{\phi}^2 - \frac{1}{2} a (\nabla \phi)^2 . \quad (6)$$

This implies the classical wave equation

$$\ddot{\phi} + 3 \frac{\dot{a}}{a} \dot{\phi} - \frac{1}{a^2} \nabla^2 \phi = 0 . \quad (7)$$

It is convenient to work in Fourier space, with components

$$\phi_{\mathbf{k}}(t) = \frac{1}{(2\pi)^{3/2}} \int d^3 \mathbf{x} \phi(\mathbf{x}, t) e^{-i\mathbf{k} \cdot \mathbf{x}} .$$

It is usual to take $a_0 = 1$ today, at time t_0 . Physical wavelengths are then given by $\lambda_{\text{phys}} = a(t)\lambda$, where $\lambda = 2\pi/k$ is the proper wavelength today and $k = |\mathbf{k}|$ is the corresponding wave number.

We may write $\phi_{\mathbf{k}}$ in terms of its real and imaginary parts,

$$\phi_{\mathbf{k}} = \frac{\sqrt{V}}{(2\pi)^{3/2}} (q_{\mathbf{k}1} + iq_{\mathbf{k}2}) ,$$

where V is a box normalisation volume. The real variables $q_{\mathbf{k}r}$ ($r = 1, 2$) are subject to the constraint $q_{\mathbf{k}1} = q_{-\mathbf{k}1}$, $q_{\mathbf{k}2} = -q_{-\mathbf{k}2}$ (since ϕ is real). In terms of these variables the Lagrangian $L = \int d^3\mathbf{x} \mathcal{L}$ reads

$$L = \sum_{\mathbf{k}r} \frac{1}{2} (a^3 \dot{q}_{\mathbf{k}r}^2 - ak^2 q_{\mathbf{k}r}^2) .$$

We then have canonical momenta $\pi_{\mathbf{k}r} \equiv \partial L / \partial \dot{q}_{\mathbf{k}r} = a^3 \dot{q}_{\mathbf{k}r}$ and the Hamiltonian becomes

$$H = \sum_{\mathbf{k}r} \left(\frac{1}{2a^3} \pi_{\mathbf{k}r}^2 + \frac{1}{2} ak^2 q_{\mathbf{k}r}^2 \right) .$$

This system is readily quantised. The Schrödinger equation for $\Psi = \Psi[q_{\mathbf{k}r}, t]$ reads

$$i \frac{\partial \Psi}{\partial t} = \sum_{\mathbf{k}r} \left(-\frac{1}{2a^3} \frac{\partial^2}{\partial q_{\mathbf{k}r}^2} + \frac{1}{2} ak^2 q_{\mathbf{k}r}^2 \right) \Psi . \quad (8)$$

This implies the continuity equation

$$\frac{\partial |\Psi|^2}{\partial t} + \sum_{\mathbf{k}r} \frac{\partial}{\partial q_{\mathbf{k}r}} \left(|\Psi|^2 \frac{1}{a^3} \frac{\partial S}{\partial q_{\mathbf{k}r}} \right) = 0 ,$$

from which we may identify the de Broglie velocities

$$\frac{dq_{\mathbf{k}r}}{dt} = \frac{1}{a^3} \frac{\partial S}{\partial q_{\mathbf{k}r}} = \frac{1}{a^3} \text{Im} \frac{1}{\Psi} \frac{\partial \Psi}{\partial q_{\mathbf{k}r}} \quad (9)$$

(with $\Psi = |\Psi| e^{iS}$). We may now consider a theoretical ensemble of fields with the same wave functional Ψ . The time evolution of each field is determined by (9). The time evolution of an arbitrary distribution $P[q_{\mathbf{k}r}, t]$ of fields will therefore be determined by

$$\frac{\partial P}{\partial t} + \sum_{\mathbf{k}r} \frac{\partial}{\partial q_{\mathbf{k}r}} \left(P \frac{1}{a^3} \frac{\partial S}{\partial q_{\mathbf{k}r}} \right) = 0 . \quad (10)$$

As usual in pilot-wave theory, if $P[q_{\mathbf{k}r}, t_i] = |\Psi[q_{\mathbf{k}r}, t_i]|^2$ then $P[q_{\mathbf{k}r}, t] = |\Psi[q_{\mathbf{k}r}, t]|^2$ for all t . Whereas if $P[q_{\mathbf{k}r}, t_i] \neq |\Psi[q_{\mathbf{k}r}, t_i]|^2$ then for as long as P remains in nonequilibrium the statistics will generally differ from those predicted by the Born rule.

This pilot-wave model has been applied to inflationary cosmology [18, 19, 20]. We have assumed that there is a preferred foliation of spacetime with time function t . (Note that spatial homogeneity is not required. A similar construction may be given in any globally-hyperbolic spacetime by choosing a preferred foliation [49, 36, 41].)

Let us now focus on the case of a decoupled (that is, unentangled) mode \mathbf{k} . If Ψ takes the form $\Psi = \psi_{\mathbf{k}}(q_{\mathbf{k}1}, q_{\mathbf{k}2}, t)\varkappa$, where \varkappa depends only on degrees of

freedom for modes $\mathbf{k}' \neq \mathbf{k}$, we may write an independent dynamics for the mode. Dropping the index \mathbf{k} hereafter, and introducing the time-dependent quantities

$$m = a^3, \quad \omega = k/a, \quad (11)$$

it follows from (8) that the wave function $\psi = \psi(q_1, q_2, t)$ satisfies a Schrödinger equation

$$i \frac{\partial \psi}{\partial t} = \sum_{r=1,2} \left(-\frac{1}{2m} \partial_r^2 + \frac{1}{2} m \omega^2 q_r^2 \right) \psi, \quad (12)$$

while from (9) it follows that de Broglie's equation of motion for the configuration (q_1, q_2) reads

$$\dot{q}_r = \frac{1}{m} \text{Im} \frac{\partial_r \psi}{\psi} \quad (13)$$

(with $\partial_r \equiv \partial/\partial q_r$). The marginal distribution $\rho = \rho(q_1, q_2, t)$ for the mode will then evolve according to

$$\frac{\partial \rho}{\partial t} + \sum_{r=1,2} \partial_r \left(\rho \frac{1}{m} \text{Im} \frac{\partial_r \psi}{\psi} \right) = 0. \quad (14)$$

Equations (12), (13) and (14) are formally the same as those of pilot-wave dynamics for a nonrelativistic particle with a time-dependent mass $m = a^3$ and moving (in the $q_1 - q_2$ plane) in a harmonic oscillator potential with time-dependent angular frequency $\omega = k/a$. Thus, for a decoupled field mode, we may discuss relaxation (and its suppression) in terms of relaxation for a nonrelativistic two-dimensional harmonic oscillator with a time-dependent mass and frequency [18, 19, 41].

In a case where m and ω are constant, it is already known that the equations (12)–(14) generate an efficient relaxation to equilibrium. How will relaxation be affected by a time-dependent scale factor $a(t)$? The answer depends on how the physical wavelength λ_{phys} compares with the Hubble radius H^{-1} .

In the short-wavelength limit we should recover the equations for a decoupled mode \mathbf{k} on Minkowski spacetime – since, roughly speaking, the timescale $\Delta t \propto \lambda_{\text{phys}}$ over which ψ evolves will be much smaller than the expansion timescale $H^{-1} \equiv a/\dot{a}$ [18]. More precisely, the short-wavelength limit may be defined by $\lambda_{\text{phys}} \ll \Delta n \cdot H^{-1}$, where $n = n_1 + n_2$ is the sum of the occupation numbers (for the modes $r = 1, 2$) and Δn is the quantum spread thereof. If we consider an evolution over timescales $\Delta t \equiv 1/\Delta E \ll H^{-1}$ (for which a is approximately constant and where ΔE is the quantum energy spread), then the equations reduce to those for a decoupled mode on Minkowski spacetime – or, to those for a two-dimensional oscillator with constant mass m and constant angular frequency ω [19, 41]. Thus, in the far sub-Hubble regime we may deduce that, if the mode \mathbf{k} is in a superposition of many different states of definite occupation number, then an initial nonequilibrium distribution $\rho \neq |\psi|^2$ will rapidly relax to equilibrium (on a coarse-grained level) – just as occurs for nonrelativistic particles moving in two dimensions [30, 32, 37, 38, 39, 40].

In contrast, in the long-wavelength limit – which may be defined by $\lambda_{\text{phys}} \gg \Delta n \cdot H^{-1}$ – we expect that the wave function ψ will be approximately static (or ‘frozen’) over timescales $\sim H^{-1}$. A similar ‘freezing’ over timescales $\sim H^{-1}$ is then expected both for the trajectories $(q_1(t), q_2(t))$ and for arbitrary nonequilibrium distributions $\rho \neq |\psi|^2$ [18, 19]. This is of course reminiscent of the freezing of super-Hubble modes in the theory of cosmological perturbations [50, 1, 4]. In both cases, the freezing occurs for dynamical reasons.

This simple reasoning suggests that relaxation to quantum equilibrium will take place as usual in the far sub-Hubble regime but can be suppressed in the far super-Hubble regime [18]. This expectation is supported by a general upper bound on the mean displacement of trajectories in configuration space, which implies a suppression of relaxation provided a certain ‘freezing inequality’ is satisfied [19, 41]. The inequality is difficult to evaluate since it depends on the time evolution of the quantum state; even so, the inequality can be satisfied only for super-Hubble modes.

Here we construct an exactly-solvable model of relaxation suppression in the super-Hubble regime. As we shall see, the results broadly confirm the general expectations [18, 19, 20, 41].

3 Exact solution for the wave function

We need to solve the Schrödinger equation (12) for the wave function $\psi = \psi(q_1, q_2, t)$. We may write the Hamiltonian as $\hat{H} = \hat{H}_1 + \hat{H}_2$ where

$$\hat{H}_r = -\frac{1}{2m} \partial_r^2 + \frac{1}{2} m \omega^2 q_r^2 . \quad (15)$$

The Hamiltonian is of course time dependent, $\hat{H} = \hat{H}(t)$. We shall be interested in a radiation-dominated expansion, over a time interval (t_i, t_f) , with scale factor $a = a_i(t/t_i)^{1/2}$.

To solve this problem we may expand the initial wave function (at time $t = t_i$) in terms of the instantaneous eigenstates $\Phi_{n_1}(q_1)\Phi_{n_2}(q_2)$ of the initial Hamiltonian $\hat{H}(t_i)$:

$$\psi(q_1, q_2, t_i) = \sum_{n_1 n_2} c_{n_1 n_2}(t_i) \Phi_{n_1}(q_1) \Phi_{n_2}(q_2) , \quad (16)$$

where $\Phi_{n_r}(q_r)$ is the n_r th eigenstate of the initial one-dimensional Hamiltonian $\hat{H}_r(t_i)$. If we know how the initial wave function $\psi_{n_r}(q_r, t_i) = \Phi_{n_r}(q_r)$ evolves under the one-dimensional Schrödinger equation

$$i \frac{\partial \psi_{n_r}(q_r, t)}{\partial t} = \hat{H}_r(t) \psi_{n_r}(q_r, t) \quad (17)$$

then we will have the solution to the full two-dimensional problem. The exact solution for the wave function may then be written as

$$\psi(q_1, q_2, t) = \sum_{n_1 n_2} c_{n_1 n_2}(t_i) \psi_{n_1}(q_1, t) \psi_{n_2}(q_2, t) . \quad (18)$$

The problem is therefore reduced to solving (17) for all of the wave functions $\psi_{n_r} = \psi_{n_r}(q_r, t)$ with the initial conditions $\psi_{n_r}(q_r, t_i) = \Phi_{n_r}(q_r)$. A partial answer to this problem can be found in ref. [51] (building on the early work of Lewis and Riesenfeld [52, 53]), where it is shown that the required wave functions take the form

$$\begin{aligned} \psi_{n_r}(q_r, t) = & \frac{1}{\sqrt{2^{n_r} n_r!}} \left(\frac{\omega_i}{\pi g_-(t)} \right)^{\frac{1}{4}} \exp \left(-i \frac{g_0(t)}{2g_-(t)} q_r^2 \right) \cdot \exp \left(-i \left(n_r + \frac{1}{2} \right) \int_{t_i}^t dt' \frac{\omega_i}{m(t') g_-(t')} \right) \\ & \times \exp \left(-\frac{\omega_i}{2g_-(t)} q_r^2 \right) \cdot \mathcal{H}_{n_r} \left(\sqrt{\frac{\omega_i}{g_-(t)}} q_r \right) . \end{aligned} \quad (19)$$

Here $\omega_i = \omega(t_i)$, the \mathcal{H}_n are Hermite polynomials, and the functions $g_-(t)$, $g_0(t)$ and $g_+(t)$ satisfy the ordinary differential equations (valid for general $a(t)$)

$$\dot{g}_- = -2 \frac{g_0}{m} \quad (20)$$

$$\dot{g}_0 = m \omega^2 g_- - \frac{g_+}{m} \quad (21)$$

$$\dot{g}_+ = 2m \omega^2 g_0 \quad (22)$$

with the initial conditions

$$g_-(t_i) = \frac{1}{m_i} , \quad g_0(t_i) = 0 , \quad g_+(t_i) = m_i \omega_i^2 \quad (23)$$

(where $m_i = m(t_i)$). According to the analysis of ref. [51], the most general solution for $g_-(t)$ takes the form

$$g_- = c_1 f_1^2 + c_2 f_1 f_2 + c_3 f_2^2 , \quad (24)$$

where $f_1(t)$ and $f_2(t)$ are two independent solutions of the classical equation of motion

$$\ddot{f} + \frac{\dot{m}}{m} \dot{f} + \omega^2 f = 0 . \quad (25)$$

If two independent solutions of (25) can be found, we will have an expression for g_- involving the three constants c_1 , c_2 and c_3 . The functions g_0 , g_+ can then be determined from g_- by means of (20) and (21). Finally, the constants c_1 , c_2 and c_3 are fixed by the initial conditions (23).

Equation (25) is of course the well-known equation for modes $\phi(\mathbf{x}, t) \propto f_1(t) e^{i\mathbf{k} \cdot \mathbf{x}}$ of the wave equation (7). For any power law $a \propto t^p$ it has solutions that are Bessel functions [4]. For definiteness, we shall restrict ourselves to the case $a \propto t^{1/2}$.

3.1 Solution for a radiation-dominated expansion

We require the solutions (19) for a radiation-dominated expansion $a = a_i(t/t_i)^{1/2}$. To this end we must first obtain two independent solutions of (25). With $m = a^3 = a_i^3(t/t_i)^{3/2}$ and $\omega = k/a = (k/a_i)(t_i/t)^{1/2}$, equation (25) becomes

$$\ddot{f}(t) + \frac{3}{2t} \dot{f}(t) + \frac{\varepsilon}{t} f(t) = 0 , \quad (26)$$

where it is useful to define the parameter

$$\varepsilon \equiv \left(\frac{t_i}{a_i^2} \right) k^2 \quad (27)$$

(so that $\omega^2 = \varepsilon/t$). The solutions to (26) are

$$f_1 = \frac{1}{\sqrt{t}} \cos 2(\sqrt{\varepsilon t} - \sqrt{\varepsilon t_i}), \quad f_2 = \frac{1}{\sqrt{t}} \sin 2(\sqrt{\varepsilon t} - \sqrt{\varepsilon t_i}). \quad (28)$$

From (24) it then follows that

$$g_- = \frac{c_1}{t} \cos^2 2(\sqrt{\varepsilon t} - \sqrt{\varepsilon t_i}) + \frac{c_2}{t} \sin 2(\sqrt{\varepsilon t} - \sqrt{\varepsilon t_i}) \cdot \cos 2(\sqrt{\varepsilon t} - \sqrt{\varepsilon t_i}) + \frac{c_3}{t} \sin^2 2(\sqrt{\varepsilon t} - \sqrt{\varepsilon t_i}). \quad (29)$$

This can be rewritten as

$$g_- = \frac{1}{t} \left(A + B \cos 4(\sqrt{\varepsilon t} - \sqrt{\varepsilon t_i}) + C \sin 4(\sqrt{\varepsilon t} - \sqrt{\varepsilon t_i}) \right) \quad (30)$$

where A , B and C are three constants that need to be determined.

To fix A , B and C , we first use (20) and (21) to calculate g_0 , g_+ from g_- and we then impose the initial conditions (23). We find that

$$A = \frac{1 + 8\varepsilon t_i}{8a_i^3 \varepsilon}, \quad B = -\frac{1}{8a_i^3 \varepsilon}, \quad C = \frac{\sqrt{\varepsilon t_i}}{2a_i^3 \varepsilon}. \quad (31)$$

Thus we have

$$g_-(t) = \frac{1}{8a_i^3 \varepsilon t} \left[(1 + 8\varepsilon t_i) - \cos 4(\sqrt{\varepsilon t} - \sqrt{\varepsilon t_i}) + 4\sqrt{\varepsilon t_i} \sin 4(\sqrt{\varepsilon t} - \sqrt{\varepsilon t_i}) \right]. \quad (32)$$

We also find that

$$g_0(t) = \frac{1}{16\varepsilon t_i \sqrt{t_i t}} \left(\begin{aligned} &(1 + 8\varepsilon t_i) - (1 + 8\sqrt{\varepsilon t_i} \sqrt{\varepsilon t}) \cos 4(\sqrt{\varepsilon t} - \sqrt{\varepsilon t_i}) \\ &+ 2(2\sqrt{\varepsilon t_i} - \sqrt{\varepsilon t}) \sin 4(\sqrt{\varepsilon t} - \sqrt{\varepsilon t_i}) \end{aligned} \right)$$

Finally, to have the complete expression for the wave functions (19) we must evaluate the integral

$$\Theta(t) \equiv \int_{t_i}^t dt' \frac{\omega_i}{m(t')g_-(t')}. \quad (33)$$

Using $m = a^3$ and (30), the integral takes the form

$$\Theta = \frac{k t_i^{3/2}}{a_i a_i^3} \int_{t_i}^t \frac{dt'}{\sqrt{t'} A + B \cos 4(\sqrt{\varepsilon t'} - \sqrt{\varepsilon t_i}) + C \sin 4(\sqrt{\varepsilon t'} - \sqrt{\varepsilon t_i})}. \quad (34)$$

With the change of variables $\phi = 4(\sqrt{\varepsilon t'} - \sqrt{\varepsilon t_i})$ we have

$$\Theta = \frac{k t_i^{3/2}}{2a_i^4 \sqrt{\varepsilon}} \int_0^{4(\sqrt{\varepsilon t} - \sqrt{\varepsilon t_i})} d\phi \frac{1}{A + B \cos \phi + C \sin \phi}. \quad (35)$$

This integral may be evaluated, with a result that depends on the relation between A , B and C . From (31) we have $A^2 > B^2 + C^2$. In this case one has (ref. [54], p.174)

$$\int d\phi \frac{1}{A + B \cos \phi + C \sin \phi} = \frac{2}{\sqrt{A^2 - B^2 - C^2}} \tan^{-1} \frac{(A - B) \tan \frac{\phi}{2} + C}{\sqrt{A^2 - B^2 - C^2}}. \quad (36)$$

This result employs the change of variables $t = \tan \frac{\phi}{2}$, which is singular when ϕ is an odd multiple of π . Therefore the domain of integration must be cut into parts ($[0, \pi)$, $(\pi, 3\pi)$, \dots) and each time ϕ moves from one domain to the next there is an additional contribution of π which must be added to the function \tan^{-1} . Therefore the total result for Θ is

$$\begin{aligned} \Theta(t) = \tan^{-1} \left(\frac{1 + 4\varepsilon t_i}{4\varepsilon t_i} \tan(2\sqrt{\varepsilon t} - 2\sqrt{\varepsilon t_i}) + \frac{1}{2\sqrt{\varepsilon t_i}} \right) \\ + \pi \cdot \text{nint} \left(\frac{2\sqrt{\varepsilon t} - 2\sqrt{\varepsilon t_i}}{\pi} \right) - \tan^{-1} \left(\frac{1}{2\sqrt{\varepsilon t_i}} \right). \end{aligned} \quad (37)$$

(where $\text{nint}(x)$ returns the integer nearest to x).

4 Properties of the trajectories

We have an exact solution (18) for the wave function $\psi(q_1, q_2, t)$. In pilot-wave theory the actual configuration $(q_1(t), q_2(t))$ at time t evolves according to de Broglie's equation of motion (13). This yields velocities

$$\dot{q}_1 = -\frac{1}{m} \frac{g_0}{g_-} q_1 + \frac{1}{m} \sqrt{\frac{\omega_i}{g_-}} \text{Im} \left(\frac{\sum_{n_1 n_2} \tilde{c}_{n_1 n_2}(t_{ret}(t)) \mathcal{H}'_{n_1}(\sqrt{\frac{\omega_i}{g_-}} q_1) \mathcal{H}_{n_2}(\sqrt{\frac{\omega_i}{g_-}} q_2)}{\sum_{m_1 m_2} \tilde{c}_{m_1 m_2}(t_{ret}(t)) \mathcal{H}_{m_1}(\sqrt{\frac{\omega_i}{g_-}} q_1) \mathcal{H}_{m_2}(\sqrt{\frac{\omega_i}{g_-}} q_2)} \right) \quad (38)$$

and

$$\dot{q}_2 = -\frac{1}{m} \frac{g_0}{g_-} q_2 + \frac{1}{m} \sqrt{\frac{\omega_i}{g_-}} \text{Im} \left(\frac{\sum_{n_1 n_2} \tilde{c}_{n_1 n_2}(t_{ret}(t)) \mathcal{H}_{n_1}(\sqrt{\frac{\omega_i}{g_-}} q_1) \mathcal{H}'_{n_2}(\sqrt{\frac{\omega_i}{g_-}} q_2)}{\sum_{m_1 m_2} \tilde{c}_{m_1 m_2}(t_{ret}(t)) \mathcal{H}_{m_1}(\sqrt{\frac{\omega_i}{g_-}} q_1) \mathcal{H}_{m_2}(\sqrt{\frac{\omega_i}{g_-}} q_2)} \right) \quad (39)$$

(where a prime on \mathcal{H} denotes a derivative with respect to the argument). Here

$$\tilde{c}_{n_1 n_2}(t) \equiv \frac{c_{n_1 n_2}(t_i) e^{-i(t-t_i)\omega_i(n_1+n_2+1)}}{\sqrt{2^{n_1} n_1!} \sqrt{2^{n_2} n_2!}} \quad (40)$$

and we have defined the *retarded time*

$$t_{ret}(t) \equiv t_i + \int_{t_i}^t \frac{1}{m(t')g_-(t')} dt'. \quad (41)$$

This is related to $\Theta(t)$ by

$$t_{\text{ret}}(t) = t_i + \frac{1}{\omega_i} \Theta(t) . \quad (42)$$

(For a plot of the function $t_{\text{ret}} = t_{\text{ret}}(t)$, see Figure 1.)

4.1 Rescaled variables

Our wave functions $\psi_{n_r}(q_r, t)$, given by (19), have time-dependent widths that are proportional to $\sqrt{g_-}$. From the solution (32) for g_- ($\sim 1/t$), we see that the widths shrink with time as $\sim 1/\sqrt{t}$ (with an oscillatory factor as well). Because of this shrinking support it is convenient to use the rescaled variables

$$q'_r = \sqrt{\frac{\omega_i}{g_-(t)}} q_r . \quad (43)$$

Their time evolution is given by

$$\frac{dq'_r}{dt} = \sqrt{\frac{\omega_i}{g_-}} \left(\dot{q}_r - \frac{1}{2} \frac{\dot{g}_-}{g_-} q_r \right) = \sqrt{\frac{\omega_i}{g_-}} \left(\dot{q}_r + \frac{1}{m} \frac{g_0}{g_-} q_r \right) , \quad (44)$$

where we have used (20). From the respective expressions (38), (39) for \dot{q}_1, \dot{q}_2 we then find

$$\dot{q}'_1(t) = \frac{1}{m} \frac{\omega_i}{g_-} \text{Im} \left[\frac{\sum_{n_1 n_2} \tilde{c}_{n_1 n_2}(t_{\text{ret}}(t)) \mathcal{H}'_{n_1}(q'_1) \mathcal{H}_{n_2}(q'_2)}{\sum_{m_1 m_2} \tilde{c}_{m_1 m_2}(t_{\text{ret}}(t)) \mathcal{H}_{m_1}(q'_1) \mathcal{H}_{m_2}(q'_2)} \right] \quad (45)$$

and

$$\dot{q}'_2(t) = \frac{1}{m} \frac{\omega_i}{g_-} \text{Im} \left[\frac{\sum_{n_1 n_2} \tilde{c}_{n_1 n_2}(t_{\text{ret}}(t)) \mathcal{H}_{n_1}(q'_1) \mathcal{H}'_{n_2}(q'_2)}{\sum_{m_1 m_2} \tilde{c}_{m_1 m_2}(t_{\text{ret}}(t)) \mathcal{H}_{m_1}(q'_1) \mathcal{H}_{m_2}(q'_2)} \right] . \quad (46)$$

4.2 Equivalence to the standard oscillator at retarded time

We shall now show that the rescaled trajectory of the system is identical to a rescaled trajectory generated by a *standard* harmonic oscillator – with coordinates Q_r , constant mass m_i and constant frequency ω_i , and with the same initial wave function (16) at $t = t_i$ – but now with time running from t_i up to the retarded time $t_{\text{ret}}(t)$ (instead of from t_i to t). We also demonstrate a correspondence between the equilibrium states for the two systems.

For our standard harmonic oscillator we have a wave function $\psi_{\text{SHO}} = \psi_{\text{SHO}}(Q_1, Q_2, t)$ and a Schrödinger equation

$$i \frac{\partial \psi_{\text{SHO}}}{\partial t} = -\frac{1}{2m_i} \left(\frac{\partial^2}{\partial Q_1^2} + \frac{\partial^2}{\partial Q_2^2} \right) \psi_{\text{SHO}} + \frac{1}{2} m_i \omega_i^2 (Q_1^2 + Q_2^2) \psi_{\text{SHO}} . \quad (47)$$

For Q_r the de Broglie velocity field is given by

$$\dot{Q}_r = \frac{1}{m_i} \text{Im} \frac{1}{\psi_{\text{SHO}}} \frac{\partial \psi_{\text{SHO}}}{\partial Q_r} . \quad (48)$$

With an initial wave function

$$\psi_{\text{SHO}}(Q_1, Q_2, t_i) = \sum_{n_1 n_2} c_{n_1 n_2}(t_i) \Phi_{n_1}(Q_1) \Phi_{n_2}(Q_2)$$

(identical to (16) with the coordinates q_1, q_2 replaced by Q_1, Q_2), we have the solution

$$\psi_{\text{SHO}}(Q_1, Q_2, t) = \sum_{n_1 n_2} c_{n_1 n_2}(t_i) \psi_{\text{SHO } n_1}(Q_1, t) \psi_{\text{SHO } n_2}(Q_2, t) , \quad (49)$$

where now instead of (19) the functions $\psi_{\text{SHO } n_r}(Q_r, t)$ take the simple form

$$\begin{aligned} \psi_{\text{SHO } n_r}(Q_r, t) &= \frac{1}{\sqrt{2^{n_r} n_r!}} \left(\frac{m_i \omega_i}{\pi} \right)^{\frac{1}{4}} \exp \left(-i \left(n_r + \frac{1}{2} \right) \omega_i (t - t_i) \right) \\ &\times \exp \left(-\frac{m_i \omega_i}{2} Q_r^2 \right) \cdot \mathcal{H}_{n_r}(\sqrt{m_i \omega_i} Q_r) . \end{aligned} \quad (50)$$

Introducing the rescaled variable $Q'_r = \sqrt{m_i \omega_i} Q_r$ (which has the same rescaling as q'_r at $t = t_i$), it follows from (48) that the velocities $\dot{Q}'_r = \sqrt{m_i \omega_i} \dot{Q}_r$ are given by

$$\dot{Q}'_1(t) = \omega_i \text{Im} \left[\frac{\sum_{n_1 n_2} \tilde{c}_{n_1 n_2}(t) \mathcal{H}'_{n_1}(Q'_1) \mathcal{H}_{n_2}(Q'_2)}{\sum_{m_1 m_2} \tilde{c}_{m_1 m_2}(t) \mathcal{H}_{m_1}(Q'_1) \mathcal{H}_{m_2}(Q'_2)} \right] \quad (51)$$

and

$$\dot{Q}'_2(t) = \omega_i \text{Im} \left[\frac{\sum_{n_1 n_2} \tilde{c}_{n_1 n_2}(t) \mathcal{H}_{n_1}(Q'_1) \mathcal{H}'_{n_2}(Q'_2)}{\sum_{m_1 m_2} \tilde{c}_{m_1 m_2}(t) \mathcal{H}_{m_1}(Q'_1) \mathcal{H}_{m_2}(Q'_2)} \right] . \quad (52)$$

Let us now compare the velocities for q'_r and Q'_r . We have, from (45), (46) and (51), (52), the simple relationship

$$\dot{q}'_r(t)|_{q'_1=a, q'_2=b} = \frac{1}{m(t)g_-(t)} \dot{Q}'_r(t_{\text{ret}}(t))|_{Q'_1=a, Q'_2=b} \quad (53)$$

or

$$\dot{q}'_r(t)|_{q'_1=a, q'_2=b} dt = \dot{Q}'_r(t_{\text{ret}}(t))|_{Q'_1=a, Q'_2=b} dt_{\text{ret}} , \quad (54)$$

where we have used

$$dt_{\text{ret}} = \frac{1}{m(t)g_-(t)} dt . \quad (55)$$

Here $t_{\text{ret}} = t_{\text{ret}}(t)$ is the retarded time (41) ‘corresponding to’ time t , and each side of (53) or (54) is evaluated at the same point (a, b) in the respective configuration space.

The displacement of q'_r from t_i up to time t is given by

$$\delta q'_r(t, t_i) = \int_{t_i}^t \dot{q}'_r(t') dt' ,$$

while the displacement of Q'_r from t_i up to the corresponding retarded time $t_{\text{ret}}(t)$ is given by

$$\delta Q'_r(t_{\text{ret}}, t_i) = \int_{t_i}^{t_{\text{ret}}} \dot{Q}'_r(t') dt' .$$

From (54) it follows that if the two systems begin at the same corresponding points in configuration space – that is, if $(q'_1(t_i), q'_2(t_i)) = (Q'_1(t_i), Q'_2(t_i))$ – then the respective displacements over the time periods (t_i, t) and $(t_i, t_{\text{ret}}(t))$ will be equal:

$$\delta q'_r(t, t_i) = \delta Q'_r(t_{\text{ret}}, t_i) . \quad (56)$$

The result (56) shows the complete dynamical equivalence of the two systems – the field oscillator on expanding space with an effective time-dependent mass $m = a^3$ and frequency $\omega = k/a$, and the standard oscillator with constant initial mass $m_i = a_i^3$ and frequency $\omega_i = k/a_i$ – with the time t for the first system replaced by the retarded time $t_{\text{ret}}(t)$ for the second system (provided the respective coordinates q_r, Q_r are rescaled to q'_r, Q'_r).

There is also a one-to-one correspondence between the equilibrium states for the two systems. At $t = t_i$ the wave functions coincide and one system will be in equilibrium if and only if the other is. From (56) it follows that the field system on expanding space will be in equilibrium at time t if and only if the equivalent oscillator is in equilibrium at time $t_{\text{ret}}(t)$.

Let us show this explicitly. From the expressions (18) and (49) for the respective wave functions $\psi(q_1, q_2, t)$ and $\psi_{\text{SHO}}(Q_1, Q_2, t)$ we find the relation

$$\frac{g_-(t)}{\omega_i} \left(|\psi(q_1, q_2, t)|^2 \right) \Big|_{q'_1=a, q'_2=b} = \frac{1}{m_i \omega_i} \left(|\psi_{\text{SHO}}(Q_1, Q_2, t_{\text{ret}}(t))|^2 \right) \Big|_{Q'_1=a, Q'_2=b} , \quad (57)$$

with each side evaluated at corresponding rescaled points (a, b) . The left-hand side is the equilibrium distribution $\rho'_{\text{QT}}(q'_1, q'_2, t)$ for the rescaled field variables, while the right-hand side is the equilibrium distribution $\rho'_{\text{SHO QT}}(Q'_1, Q'_2, t_{\text{ret}}(t))$ for the rescaled oscillator. Thus we have

$$\rho'_{\text{QT}}(q'_1, q'_2, t) = \rho'_{\text{SHO QT}}(Q'_1, Q'_2, t_{\text{ret}}(t)) \quad (58)$$

(where it is understood that the two sides are evaluated at corresponding points). If we assume that the initial – generally nonequilibrium – distributions for the two systems are equal, $\rho(q_1, q_2, t_i) = \rho_{\text{SHO}}(Q_1, Q_2, t_i)$, then since the initial rescalings coincide the initial rescaled distributions will also be equal: $\rho'(q'_1, q'_2, t_i) = \rho'_{\text{SHO}}(Q'_1, Q'_2, t_i)$. From the correspondence (56) between the rescaled trajectories it then follows that

$$\rho'(q'_1, q'_2, t) = \rho'_{\text{SHO}}(Q'_1, Q'_2, t_{\text{ret}}(t)) \quad (59)$$

at all times t – that is, the rescaled density for the field system at time t is equal to the rescaled density for the oscillator at the retarded time $t_{\text{ret}}(t)$. From (58) and (59) we may write

$$\frac{\rho'(q'_1, q'_2, t)}{\rho'_{\text{QT}}(q'_1, q'_2, t)} = \frac{\rho'_{\text{SHO}}(Q'_1, Q'_2, t_{\text{ret}}(t))}{\rho'_{\text{SHO QT}}(Q'_1, Q'_2, t_{\text{ret}}(t))} .$$

The field system will be in equilibrium at time t (left-hand ratio equal to one) if and only if the equivalent oscillator is in equilibrium at time $t_{\text{ret}}(t)$ (right-hand ratio equal to one).

The retarded time $t_{\text{ret}} = t_{\text{ret}}(t)$ is determined by (41) for given functions $a(t)$, $g_-(t)$ on the interval (t_i, t) . For a radiation-dominated expansion, $a \propto t^{1/2}$, we have an exact solution (32) for $g_-(t)$ and the quantity $\Theta(t)$ has already been evaluated (equation (37)) so that we know the function $t_{\text{ret}}(t) = t_i + \Theta(t)/\omega_i$. Note that the functions $g_-(t)$ and $t_{\text{ret}}(t)$ depend on the wave number k of the mode but are independent of the quantum state of the mode. Because of the dynamical equivalence to the standard oscillator with retarded time, the essential physics of our system on expanding space is determined by properties of the function $t_{\text{ret}}(t)$, which is in turn determined by the function $g_-(t)$.

In the very short-time limit, $t = t_i + \Delta t$ with $\Delta t/t_i \ll 1$, we have $m \simeq m_i$ and $g_- \simeq g_-(t_i) = 1/m_i$ and so we have simply

$$t_{\text{ret}}(t) \simeq t_i + \int_{t_i}^t dt' = t .$$

At very short times the retarded time t_{ret} reduces to real time t .

5 Freezing of quantum nonequilibrium in the far super-Hubble regime

Two regimes are of particular significance: the far sub-Hubble and the far super-Hubble limits. In Section 3 we introduced the parameter $\varepsilon = (t_i/a_i^2) k^2$. Because

$$\varepsilon t = \frac{t t_i}{a_i^2} \left(\frac{2\pi}{\lambda} \right)^2 = \frac{t^2}{a^2} \left(\frac{2\pi}{\lambda} \right)^2 = \left(\frac{\pi H^{-1}}{a\lambda} \right)^2 = \left(\frac{\pi H^{-1}(t)}{\lambda_{\text{phys}}(t)} \right)^2 ,$$

we may conveniently characterise the far sub-Hubble regime (with $\lambda_{\text{phys}} \ll H^{-1}$) and the far super-Hubble regime (with $\lambda_{\text{phys}} \gg H^{-1}$) by respective large or small values of εt .

In the far sub-Hubble regime we may therefore take $\varepsilon t_i \gg 1$ (in which case we will also have $\varepsilon t \gg 1$ for all $t \geq t_i$). The factor in square brackets in (32) is then dominated by the term $8\varepsilon t_i$ and so we have

$$g_-(t) \simeq \frac{t_i}{a_i^3 t} \tag{60}$$

in the far sub-Hubble limit. To recover the Minkowski limit we must consider evolution over times $\Delta t \ll H_i^{-1} = 2t_i$ so that the scale factor remains essentially constant. Thus, setting $m \simeq a_i^3$ and using (60), at such a time $t_i + \Delta t$ the retarded time (41) will be

$$t_{\text{ret}}(t_i + \Delta t) \simeq t_i + \int_{t_i}^{t_i + \Delta t} \frac{t'}{t_i} dt' = t_i + \Delta t + \frac{(\Delta t)^2}{2t_i} \simeq t_i + \Delta t . \tag{61}$$

As expected, in the Minkowski limit the retarded time t_{ret} coincides with true time t . (This is a particular case of the short-time limit.)

For the far super-Hubble regime let us instead consider a time interval (t_i, t_f) during which $\varepsilon t \ll 1$. (We could simply set $\varepsilon t_f \ll 1$, in which case we will also have $\varepsilon t \ll 1$ for all $t \leq t_f$.) From (32) we find that for $\varepsilon t \ll 1$ the function $g_-(t)$ takes the constant form

$$g_-(t) \approx \frac{1}{a_i^3} = \frac{1}{m_i}. \quad (62)$$

Inserting (62) into (41), and writing $a = a_i(t/t_i)^{1/2}$, we find that in the far super-Hubble regime the retarded time is given by

$$t_{\text{ret}}(t) \simeq t_i + \int_{t_i}^t (t_i/t')^{3/2} dt' = t_i + 2t_i \left(1 - \sqrt{\frac{t_i}{t}}\right). \quad (63)$$

In the short-time limit, $t = t_i + \Delta t$ with $\Delta t \ll 2t_i$, this again reduces to

$$t_{\text{ret}}(t) \simeq t_i + \Delta t. \quad (64)$$

However, in the long-time limit with $t_f \gg t_i$ we now have

$$t_{\text{ret}}(t_f) \simeq 3t_i. \quad (65)$$

This remarkable result may be stated as follows: in the far super-Hubble regime, the long-time evolution of a field mode on an interval (t_i, t_f) with $t_f \gg t_i$ is equivalent to the time evolution of a standard harmonic oscillator on the limited time interval $(t_i, t_{\text{ret}}(t_f)) = (t_i, 3t_i)$ (with appropriate rescaling of the coordinates). In effect, *the ‘equivalent standard oscillator’ evolves over just one Hubble time $H^{-1}(t_i) = 2t_i$.*

It is now very simple to deduce that, if the equivalent standard oscillator has a relaxation timescale τ that is larger than $2t_i$ – so that equilibrium is not reached on the limited time interval $(t_i, 3t_i)$ – then the real field system will never reach equilibrium, not even for $t_f \gg t_i$ (for as long as the mode remains in the far super-Hubble regime). Thus, in appropriate conditions, quantum nonequilibrium will be ‘frozen’ for super-Hubble modes.

We have reduced the question of relaxation on expanding space to the much simpler question of relaxation for an equivalent standard oscillator. For the standard (two-dimensional) oscillator it is straightforward to study the relaxation timescale τ numerically. Analogous studies have already been carried out for a particle in a two-dimensional box, for initial wave functions that are superpositions of the first M energy eigenstates [39]. There it was found that the coarse-grained H -function \bar{H} decays approximately exponentially, $\bar{H}(t) \approx \bar{H}(t_i) \exp(-(t - t_i)/\tau)$, with a timescale $\tau \propto 1/M$ that scales (approximately) inversely with M . We expect to find comparable behaviour for the oscillator – though with a somewhat different scaling of τ with M for this different system. As the number M of energy states in the superposition

increases, the relaxation timescale τ for the oscillator will certainly decrease (owing to the increasing complexity of the de Broglie velocity field). For M larger than some critical value M_{\max} we will have $\tau \lesssim 2t_i$ and we may deduce that the equivalent field system will relax. If instead $M < M_{\max}$ we will have $\tau \gtrsim 2t_i$ and the field system will never reach equilibrium. (A detailed numerical study of relaxation for the standard oscillator, and of the scaling of τ with M , will be presented elsewhere [55].)

The above conclusions agree at least qualitatively with the analysis given in refs. [19, 41]. There it is shown that there is an upper bound on the ratio $\langle |\delta q_r(t_f)| \rangle_{\text{QT}} / \Delta_r(t_f)$,

$$\frac{\langle |\delta q_r(t_f)| \rangle_{\text{QT}}}{\Delta_r(t_f)} < 4 \sqrt{a_f^3 \langle \hat{H}_r \rangle_f} \int_{t_i}^{t_f} dt \sqrt{\langle \hat{H}_r \rangle} / a^3, \quad (66)$$

where $\langle |\delta q_r(t_f)| \rangle_{\text{QT}}$ is the (equilibrium) mean displacement of the trajectories over the time interval (t_i, t_f) and $\Delta_r(t_f) \equiv (1/2)(1/\Delta\pi_r)$ is the characteristic lengthscale of the equilibrium distribution in configuration space at time t_f (where $\Delta\pi_r$ is the quantum-theoretical spread for the canonical momentum operator $\hat{\pi}_r$). In general, relaxation can occur only if the trajectories move over distances that are at least comparable to Δ_r . For super-Hubble modes the right-hand side of (66) can be smaller than one – in which case relaxation will be suppressed, since most of the trajectories will not move far enough for relaxation to occur [19, 41]. On the other hand, clearly, the right-hand side of (66) can be large for a quantum state with a sufficiently large mean Hamiltonian $\langle \hat{H}_r \rangle$, in which case no relaxation suppression can be deduced.

6 Suppression of quantum noise at super-Hubble wavelengths

The above results provide a mechanism whereby quantum noise can be suppressed at super-Hubble wavelengths. If we assume that the initial nonequilibrium distribution has a subquantum width, then under standard relaxation the distribution evolves towards the Born rule and the width approaches the standard quantum width. But in an expanding universe such relaxation can be delayed – in accordance with the retarded time $t_{\text{ret}}(t)$ – or even completely frozen (in the far super-Hubble regime, as we saw in Section 5). In effect, as far as relaxation is concerned, over a time t it is as if only a time $t_{\text{ret}}(t) < t$ has actually passed. Therefore in general we expect that the actual width of the relaxing distribution will grow more slowly and take longer to reach the quantum value – or never reach it at all.

It is instructive to consider a numerical simulation that illustrates the retardation effect.

We take an initial wave function that is a superposition

$$\psi(q_1, q_2, t_i) = \frac{1}{\sqrt{M}} \sum_{n_1=0}^{\sqrt{M}-1} \sum_{n_2=0}^{\sqrt{M}-1} e^{i\theta_{n_1 n_2}} \Phi_{n_1}(q_1) \Phi_{n_2}(q_2)$$

of instantaneous energy eigenstates $\Phi_{n_1} \Phi_{n_2}$ of the initial Hamiltonian, with coefficients $c_{n_1 n_2}(t_i) = (1/\sqrt{M})e^{i\theta_{n_1 n_2}}$ of equal amplitude and with randomly-chosen initial phases $\theta_{n_1 n_2}$. (For simplicity the quantum numbers n_1, n_2 are taken to have the same range; the number M of modes is then restricted to be the square of an integer.) As we saw in Section 3, the wave function at time t is then

$$\psi(q_1, q_2, t) = \frac{1}{\sqrt{M}} \sum_{n_1=0}^{\sqrt{M}-1} \sum_{n_2=0}^{\sqrt{M}-1} e^{i\theta_{n_1 n_2}} \psi_{n_1}(q_1, t) \psi_{n_2}(q_2, t),$$

where the exact solution for $\psi_n(q, t)$ is given by (19).

The quantum equilibrium distribution at time t is given by $\rho_{\text{QT}}(q_1, q_2, t) = |\psi(q_1, q_2, t)|^2$. The actual probability density at the initial time t_i is taken to be

$$\rho(q_1, q_2, t_i) = |\Phi_0(q_1) \Phi_0(q_2)|^2 = \frac{\omega_i m_i}{\pi} e^{-m_i \omega_i q_1^2} e^{-m_i \omega_i q_2^2}. \quad (67)$$

This is equal to the equilibrium density for the quantum-theoretical ground state $\Phi_0(q_1) \Phi_0(q_2)$. We choose this particular initial distribution purely on grounds of simplicity. Clearly $\rho(q_1, q_2, t_i) \neq |\psi(q_1, q_2, t_i)|^2$ and the initial state is far from equilibrium. By calculating the de Broglie-Bohm trajectories $(q_1(t), q_2(t))$ numerically – using de Broglie’s equation of motion (13) – we may calculate the time evolution $\rho(q_1, q_2, t)$ of the actual distribution and study whether or not it approaches the equilibrium distribution $|\psi(q_1, q_2, t)|^2$ (on a coarse-grained level).

Because of the decreasing width of the solution (19), the support of $|\psi(q_1, q_2, t)|^2$ in the $q_1 - q_2$ plane shrinks with time. When plotting the distributions it is therefore convenient to use the rescaled variables $q'_r = \sqrt{\omega_i/g_-(t)} q_r$ (with $g_-(t_i) = 1/m_i$ and where g_- decreases with time). The equilibrium probability density in the $q'_1 - q'_2$ plane is then given by

$$\rho'_{\text{QT}}(q'_1, q'_2, t) = \frac{g_-(t)}{\omega_i} |\psi(q_1, q_2, t)|^2. \quad (68)$$

In terms of the rescaled variables $q'_r = \sqrt{m_i \omega_i} q_r$ at $t = t_i$ we have an initial nonequilibrium density

$$\rho'(q'_1, q'_2, t_i) = \frac{1}{\omega_i m_i} \rho(q_1, q_2, t_i) = \frac{1}{\pi} e^{-(q'_1)^2} e^{-(q'_2)^2}. \quad (69)$$

At later times t the actual density in the $q'_1 - q'_2$ plane is

$$\rho'(q'_1, q'_2, t) = \frac{g_-(t)}{\omega_i} \rho(q_1, q_2, t). \quad (70)$$

During a radiation-dominated expansion, a mode that begins with a super-Hubble wavelength (that is, with a physical wavelength $\lambda_{\text{phys}}(t_i) > H_i^{-1}$) will enter the Hubble radius at a later time t_{enter} that is determined by $\lambda_{\text{phys}}(t_{\text{enter}}) = H^{-1}(t_{\text{enter}})$. Thereafter the mode will acquire a sub-Hubble wavelength (that is, $\lambda_{\text{phys}}(t) < H^{-1}(t)$). Here $\lambda_{\text{phys}}(t) = a(t)\lambda$, where the comoving wavelength λ is equal to the physical wavelength at a time t_0 such that $a_0 = 1$ (often taken to be the time today).

We are particularly interested in modes that begin outside the Hubble radius. Let us consider the evolution of such a mode during the entire super-Hubble era – that is, from an initial time t_i until the time t_{enter} . For the purposes of a numerical computation we have found it convenient to take $t_i = 10^{-4}$ and $t_0 = 1$. We then have $a_i = 10^{-2}$. If we choose $\lambda = 0.2$ (or $k = 2\pi/\lambda = 10\pi$) then $\lambda_{\text{phys}}(t_i) = a_i\lambda = 2 \times 10^{-3}$ and $H_i^{-1} = 2t_i = 2 \times 10^{-4}$. At the initial time the mode is outside the Hubble radius by one order of magnitude. Mode entry occurs at $t_{\text{enter}} = 10^{-2}$. (These chosen values are not intended to have any particular cosmological significance, they are for numerical convenience and illustration only.)

The equivalence theorem of Section 4 tells us that the time evolution of the real system on expanding space, over the time interval (t_i, t_{enter}) , may be obtained by evolving the equivalent standard oscillator (with the same initial conditions for the wave function and nonequilibrium distribution) over the time interval $(t_i, t_{\text{ret}}(t_{\text{enter}}))$ – where $t_{\text{ret}}(t)$ is the retarded time corresponding to real time t . The required values of t_{ret} may be obtained from the analytical result (37) for Θ , where $t_{\text{ret}}(t) = t_i + \Theta(t)/\omega_i$. A plot of the required function $t_{\text{ret}}(t)$ – for the above values of the parameters t_i, a_i, k and over the time interval (t_i, t_{enter}) – is given in Figure 1. (For this plot the parameter ε is equal to $100\pi^2$.)

The time evolution of the equivalent standard oscillator may be obtained by straightforward numerical simulation. We employ the ‘backtracking’ method of ref. [37], which uses the conserved ratio ρ'/ρ'_{QT} along trajectories to construct ρ' on a uniform grid at each time t . Our grid consists of 1000×1000 points. We impose a precision of 0.01 on the backtracked trajectories (compared to a linear scale of ~ 10 for the support of the distributions, and where ρ'_{QT} displays structure on lengthscales down to ~ 1). The evolving density ρ' develops an extremely irregular fine-grained structure, with rapid variations over very short distances (cf. figure 6 of ref. [37]). The density may be averaged over coarse-graining cells, with a coarse-grained value assigned to the centre of each cell. It is convenient to plot a ‘smoothed’ density $\tilde{\rho}'$ obtained by coarse-graining with overlapping cells [37].³

In Figure 2 we show the result of such a simulation for the case of 25 modes ($M = 25$). The top row shows the initial (smoothed) actual distribution $\tilde{\rho}'(t_i)$ on the left-hand side and the initial (smoothed) equilibrium distribution $\tilde{\rho}'_{\text{QT}}(t_i)$ on the right-hand side. The support of $\tilde{\rho}'(t_i)$ is considerably narrower than the

³The plots in Figures 2 and 3 employ 96×96 overlapping cells each with 50×50 grid points. The cells have side $\varepsilon = 0.5$. For a given cell, shifting it along either axis by a distance equal to 20% of ε generates a neighbouring cell.

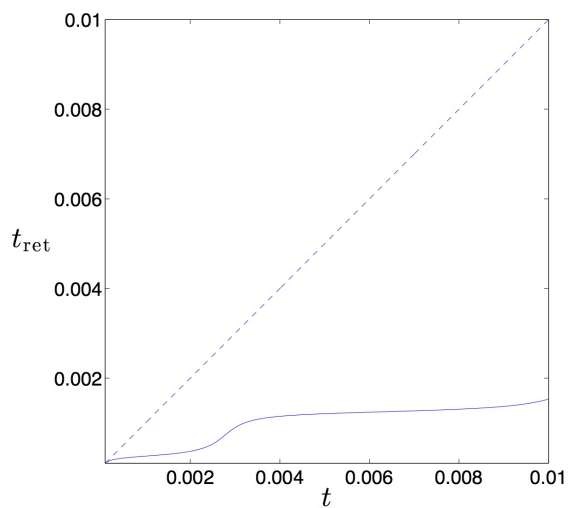


Figure 1: Plot of the retarded time $t_{\text{ret}} = t_{\text{ret}}(t)$ (solid line) for t on the interval (t_i, t_{enter}) . The dotted line is a plot of real time t . The function $t_{\text{ret}}(t)$ is given in terms of $\Theta(t)$ by $t_{\text{ret}}(t) = t_i + \Theta(t)/\omega_i$ where $\Theta(t)$ is given by equation (37). We have chosen parameters $t_i = 10^{-4}$, $a_i = 10^{-2}$ and $k = 10\pi$ (so that $\varepsilon = 100\pi^2$).

support of $\tilde{\rho}'_{\text{QT}}(t_i)$. The second row shows the (smoothed) distributions at an intermediate retarded time $t_{\text{ret}} = t_{\text{ret}}(0.5t_{\text{enter}}) = 1.21 \times 10^{-3}$, while the third row shows these at $t_{\text{ret}} = t_{\text{ret}}(t_{\text{enter}}) = 1.53 \times 10^{-3}$. The three times t_i , $t_{\text{ret}}(0.5t_{\text{enter}})$, $t_{\text{ret}}(t_{\text{enter}})$ for the equivalent oscillator correspond to the times t_i , $0.5t_{\text{enter}}$, t_{enter} for the real system on expanding space. As is plain from the figure, the support of $\tilde{\rho}'$ spreads out – at least initially – while the support of $\tilde{\rho}'_{\text{QT}}$ remains about the same (with the rescaled coordinates). However, over the time interval considered, the support of $\tilde{\rho}'$ remains significantly narrower than the support of $\tilde{\rho}'_{\text{QT}}$. There has clearly been only a partial relaxation towards equilibrium (as will be quantified below using the coarse-grained H -function).

Let us contrast this result with a simulation for the same standard oscillator, with the same initial conditions, but evolved up to a time $t = t_{\text{enter}} = 10^{-2}$. Physically, this would correspond to the time evolution of the real system with no spatial expansion (that is, with $a = 1$ for all t so that $t_{\text{ret}}(t) = t$). The results are shown in Figure 3. The first row shows the same initial conditions as before. The second and third rows show the (smoothed) distributions at the respective times $t = 0.5t_{\text{enter}}$ and $t = t_{\text{enter}}$. The results speak for themselves. Already by $t = 0.5t_{\text{enter}}$ the actual distribution $\tilde{\rho}'$ has a support that is only slightly narrower than the support of $\tilde{\rho}'_{\text{QT}}$. At $t = t_{\text{enter}}$ there is little discernible difference between the distributions $\tilde{\rho}'$ and $\tilde{\rho}'_{\text{QT}}$ – not only in terms of the extent of their support but also as regards detailed features. There has clearly been an almost complete relaxation to equilibrium.

The approach to equilibrium may be quantified using the coarse-grained H -function

$$\bar{H} = \int \int dq'_1 dq'_2 \tilde{\rho}' \ln(\tilde{\rho}' / \tilde{\rho}'_{\text{QT}}) , \quad (71)$$

where $\tilde{\rho}'$, $\tilde{\rho}'_{\text{QT}}$ are obtained by averaging ρ' , ρ'_{QT} over (non-overlapping) coarse-graining cells. As we recalled in Section 1, this function obeys a coarse-graining H -theorem [28, 30] and provides a convenient measure of relaxation. For the above two simulations, a plot of $\ln \bar{H}$ as a function of time t is shown in Figure 4. In both cases real time runs from $t = t_i$ up to $t = t_{\text{enter}}$. In the case with no spatial expansion the \bar{H} -curve has a larger (negative) slope and ends with a smaller value – the relaxation proceeds more quickly and the final distribution comes considerably closer to equilibrium. (The early part of the time evolution shows a clear exponential decay, which then appears to tail off somewhat.⁴)

The contrast between Figures 2 and 3 – quantified by the different \bar{H} -curves in Figure 4 – provides a graphic illustration of our mechanism for the suppression of quantum noise at super-Hubble wavelengths. The effect of the spatial expansion is to *retard relaxation in the super-Hubble regime*. For an initial nonequilibrium distribution with a subquantum width, at later times the width can remain subquantum – even though, over the same time interval, almost complete relaxation would have occurred if space had not been expanding.

⁴Here we employ 20×20 non-overlapping coarse-graining cells each containing 50×50 grid points. The error bars are obtained by running the same simulation with different grids so as to obtain different samples of the highly fine-grained function ρ' .

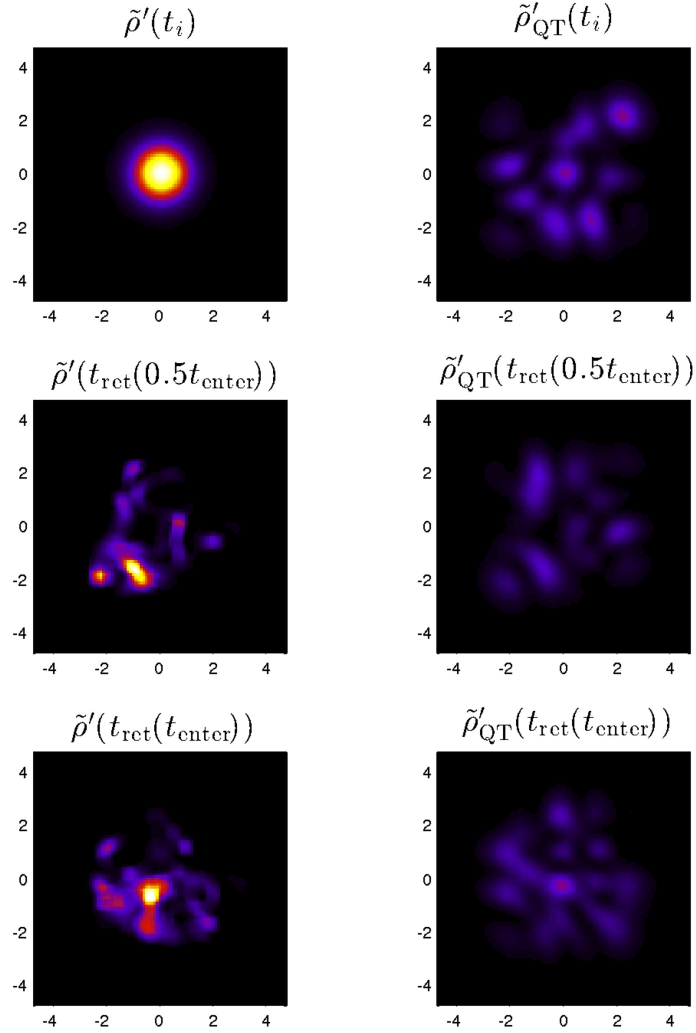


Figure 2: Time evolution of nonequilibrium on expanding space, for a superposition of 25 modes. Results for the interval (t_i, t_{enter}) are obtained by evolving the equivalent oscillator over the retarded interval $(t_i, t_{\text{ret}}(t_{\text{enter}}))$. The (smoothed) actual distribution $\tilde{\rho}'$ is displayed in the left column, the (smoothed) equilibrium distribution $\tilde{\rho}'_{QT}$ in the right column. The top row shows the distributions at the initial time t_i , the second row at an intermediate retarded time $t_{\text{ret}}(0.5t_{\text{enter}})$, and the third row at $t_{\text{ret}}(t_{\text{enter}})$. The support of $\tilde{\rho}'$ remains significantly narrower than the support of $\tilde{\rho}'_{QT}$.

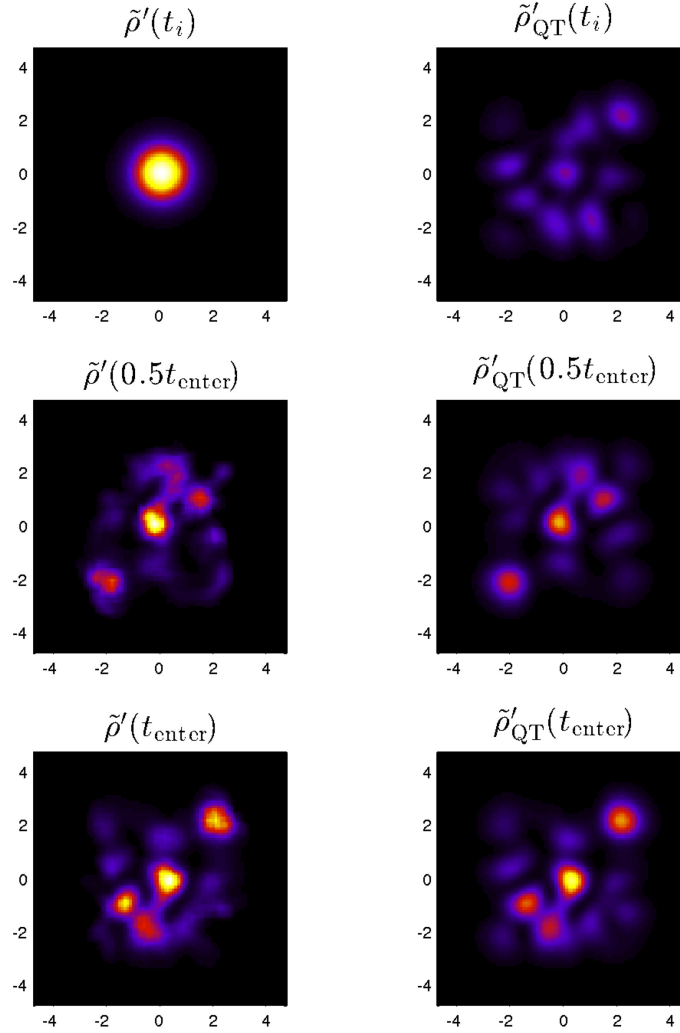


Figure 3: Time evolution of the same initial state as in Figure 2 but with no spatial expansion. The results for (t_i, t_{enter}) are now obtained simply by evolving the standard oscillator over (t_i, t_{enter}) . The top row again shows the (smoothed) distributions at the initial time t_i , the second row at the intermediate time $0.5t_{\text{enter}}$, and the third row at t_{enter} . Already at $t = 0.5t_{\text{enter}}$ the actual distribution $\tilde{\rho}'$ has a support that is only slightly narrower than the support of $\tilde{\rho}'_{\text{QT}}$. At $t = t_{\text{enter}}$ there is little discernible difference between $\tilde{\rho}'$ and $\tilde{\rho}'_{\text{QT}}$ – relaxation is almost complete.

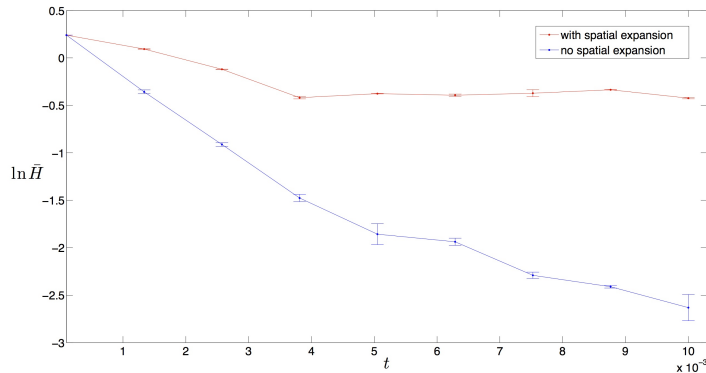


Figure 4: Plots of $\ln \bar{H}$ against time t , with spatial expansion (upper curve) and with no spatial expansion (lower curve). Real time runs from $t = t_i$ up to $t = t_{\text{enter}}$. The lower curve has a larger (negative) slope and ends with a smaller value. With no spatial expansion there is faster relaxation and the final distribution comes considerably closer to equilibrium. The difference between the two \bar{H} -curves quantifies the suppression of relaxation on expanding space in the super-Hubble regime.

7 Mechanism for a large-scale power deficit in the CMB

We have demonstrated a mechanism for the suppression of quantum noise at super-Hubble wavelengths in a radiation-dominated universe. It has been suggested that such a mechanism would generate a large-scale power deficit in the CMB in a cosmology with a radiation-dominated pre-inflationary phase [18, 19, 20]. Relaxation suppression could have occurred in the pre-inflationary era, resulting in a deficit in the inflationary spectrum above some large comoving wavelength λ_c . However, no estimate was given for the value of λ_c .

The existence of a large-scale power deficit in the CMB has recently been confirmed by the *Planck* satellite [43]. The reported statistical significance is not high (in the range $2.5\text{--}3\sigma$). It is therefore quite possible that the primordial power spectrum for a theoretical ensemble of skies is not itself anomalous, and that we have simply observed a chance fluctuation for our single sky (see Section 7.1). Even so, it is worth exploring models that predict a genuine deficit in the primordial spectrum, so as to better assess the significance of what has been observed.

We now provide a simple estimate for λ_c which depends essentially on the number N of inflationary e-folds and on the inflationary reheating temperature T_{end} . The allowed values for N and T_{end} are consistent with a cutoff λ_c corresponding to the scale of the observed power deficit. On the other hand, if N is

very large then our cutoff λ_c will be far too big to yield an observable effect on the CMB.

There are of course other possible effects that could contribute to the observed deficit (and perhaps account for it in full). For example, a deficit could arise from a period of ‘fast rolling’ for the inflaton field around the beginning of the last 65 e-folds of inflation [56]. A radiation-dominated pre-inflationary phase can also yield corrections to the quantum vacuum state during inflation, resulting in a loss of power at low l [47, 48]. Our main concern here is to show that our mechanism for quantum noise suppression on large scales could have implications for the CMB. As will be discussed further in Section 8, the development of a detailed cosmological model and comparisons with other possible effects are left for future work.

7.1 The CMB in the low- l region

We first briefly review the standard treatment of the CMB at large angular scales.

The temperature anisotropy $\Delta T(\theta, \phi) \equiv T(\theta, \phi) - \bar{T}$ of the CMB sky (where \bar{T} is the average over the sky) may be decomposed into spherical harmonics,

$$\frac{\Delta T(\theta, \phi)}{\bar{T}} = \sum_{l=2}^{\infty} \sum_{m=-l}^{+l} a_{lm} Y_{lm}(\theta, \phi). \quad (72)$$

It is usual to regard $T(\theta, \phi)$ as a single realisation of a stochastic process such that the marginal probability distribution for each coefficient a_{lm} is independent of m . This will be true if the probability distribution for $T(\theta, \phi)$ – over a theoretical ‘ensemble of skies’ – is rotationally invariant. The predicted angular power spectrum

$$C_l \equiv \langle |a_{lm}|^2 \rangle \quad (73)$$

then depends only on l (where $\langle \dots \rangle$ denotes an average over the theoretical ensemble). The quantity

$$C_l^{\text{sky}} \equiv \frac{1}{2l+1} \sum_{m=-l}^{+l} |a_{lm}|^2 \quad (74)$$

is constructed from measurements on a single sky and satisfies $\langle C_l^{\text{sky}} \rangle = C_l$. Thus C_l^{sky} gives an unbiased estimate of C_l . It has a cosmic variance $\Delta C_l^{\text{sky}} / C_l = \sqrt{2/2l+1}$. (In practice, of course, the CMB data contain additional noise and errors that must be accounted for.)

The temperature anisotropy is generated from primordial curvature perturbations $\mathcal{R}_{\mathbf{k}} \equiv (1/4) (a/k)^2 {}^{(3)}R_{\mathbf{k}}$ (where ${}^{(3)}R_{\mathbf{k}}$ is the Fourier component of the

spatial curvature scalar on comoving hypersurfaces) in accordance with the formula [57]

$$a_{lm} = \frac{i^l}{2\pi^2} \int d^3\mathbf{k} \mathcal{T}(k, l) \mathcal{R}_{\mathbf{k}} Y_{lm}(\hat{\mathbf{k}}) , \quad (75)$$

where the transfer function $\mathcal{T}(k, l)$ encodes the relevant astrophysical processes.

If the probability distribution for $\mathcal{R}_{\mathbf{k}}$ is translationally invariant it follows that $\langle \mathcal{R}_{\mathbf{k}} \mathcal{R}_{\mathbf{k}'}^* \rangle = \delta_{\mathbf{k}\mathbf{k}'} \langle |\mathcal{R}_{\mathbf{k}}|^2 \rangle$. From (75) one then obtains the expression

$$C_l = \frac{1}{2\pi^2} \int_0^\infty \frac{dk}{k} \mathcal{T}^2(k, l) \mathcal{P}_{\mathcal{R}}(k) \quad (76)$$

for the angular power spectrum in terms of the primordial power spectrum

$$\mathcal{P}_{\mathcal{R}}(k) \equiv \frac{4\pi k^3}{V} \langle |\mathcal{R}_{\mathbf{k}}|^2 \rangle \quad (77)$$

(with V a normalisation volume). This provides a link between the statistics of the primordial perturbations and the observed features in the CMB. The data for C_l are consistent with an approximately scale-free spectrum $\mathcal{P}_{\mathcal{R}}(k) \approx \text{const.}$.

At large angular scales – that is, for small values of l (say $l \lesssim 20$) – the angular power spectrum C_l is dominated by the Sachs-Wolfe effect. In this region the square of the transfer function takes the simple form [1]

$$\mathcal{T}^2(k, l) = \pi H_0^4 j_l^2(2k/H_0) , \quad (78)$$

where H_0 is the Hubble parameter today. From (76) we then have

$$C_l = \frac{H_0^4}{2\pi} \int_0^\infty \frac{dk}{k} j_l^2(2k/H_0) \mathcal{P}_{\mathcal{R}}(k) . \quad (79)$$

For an exactly scale-invariant spectrum, $\mathcal{P}_{\mathcal{R}}(k) = \text{const.}$, this yields $C_l \propto 1/l(l+1)$. (The integrated Sachs-Wolfe effect will cause a small rise in the value of $l(l+1)C_l$ at very small l .)

There were suggestions that the CMB data from the *WMAP* satellite contained anomalously low power at small l . Such claims were, however, controversial. (For a review and critical assessment based on the seven-year *WMAP* data see ref. [42].) Recently, the anomaly has been confirmed to exist in data from the *Planck* satellite [43].

The *Planck* team report a power deficit of 5–10% in the region $l \lesssim 40$, with a statistical significance in the range $2.5\text{--}3\sigma$ (depending on the estimator that is used). While the statistical significance is not high, the *Planck* team have noted the importance of finding a theoretical model that predicts a low- l deficit.

If the reported power deficit is not due to inadequate data processing or to some local astrophysical effect then it must be primordial in origin. It might be regarded as a mere random fluctuation for our single sky. Otherwise, it reflects a genuine anomaly in the primordial power spectrum $\mathcal{P}_{\mathcal{R}}(k)$ for the theoretical ensemble. To explain such an anomaly would presumably require a modification of the standard inflationary scenario – and perhaps some new physics.

7.2 Inflation with early quantum nonequilibrium

Inflationary cosmology predicts a curvature perturbation $\mathcal{R}_{\mathbf{k}}$ that may be obtained from the simple formula [1]

$$\mathcal{R}_{\mathbf{k}} = - \left[\frac{H}{\dot{\phi}_0} \phi_{\mathbf{k}} \right]_{t=t_*(k)}. \quad (80)$$

Here H is the (approximately constant) Hubble parameter of the inflating universe, while ϕ_0 and ϕ respectively denote the spatially homogeneous and inhomogeneous parts of the inflaton field. The right-hand side is evaluated at a time $t_*(k)$ taken to be a few e -folds after the exponentially-expanding physical wavelength $\lambda_{\text{phys}} = a(2\pi/k)$ of the mode exits the Hubble radius. The inflaton perturbation ϕ is defined on a spatially flat slicing, while the curvature perturbation $\mathcal{R}_{\mathbf{k}}$ is defined on the comoving slicing. Thus (80) relates quantities defined on different slicings.⁵

In an ideal Bunch-Davies vacuum the inflaton perturbations $\phi_{\mathbf{k}}$ will have (at time $t_*(k)$) a quantum-theoretical variance

$$\langle |\phi_{\mathbf{k}}|^2 \rangle_{\text{QT}} = \frac{V}{2(2\pi)^3} \frac{H^2}{k^3} \quad (81)$$

and a scale-free power spectrum

$$\mathcal{P}_{\phi}^{\text{QT}}(k) \equiv \frac{4\pi k^3}{V} \langle |\phi_{\mathbf{k}}|^2 \rangle_{\text{QT}} = \frac{H^2}{4\pi^2}. \quad (82)$$

The quantity $\langle |\phi_{\mathbf{k}}|^2 \rangle_{\text{QT}}$ is calculated from quantum field theory (for $\lambda_{\text{phys}} \gg H^{-1}$). The formula (80) then yields a quantum-theoretical power spectrum

$$\mathcal{P}_{\mathcal{R}}^{\text{QT}}(k) \equiv \frac{4\pi k^3}{V} \langle |\mathcal{R}_{\mathbf{k}}|^2 \rangle_{\text{QT}} = \left[\frac{H^2}{\dot{\phi}_0^2} \mathcal{P}_{\phi}^{\text{QT}}(k) \right]_{t_*(k)} = \frac{1}{4\pi^2} \left[\frac{H^4}{\dot{\phi}_0^2} \right]_{t_*(k)} \quad (83)$$

for $\mathcal{R}_{\mathbf{k}}$. In the slow-roll approximation we then obtain a scale-free spectrum $\mathcal{P}_{\mathcal{R}}^{\text{QT}}(k) \approx \text{const.}$. Because H and $\dot{\phi}_0$ are in fact slowly changing during the inflationary phase, there will be a small dependence of $\mathcal{P}_{\mathcal{R}}^{\text{QT}}(k)$ on k .

Now quantum nonequilibrium in the early Bunch-Davies vacuum would generally yield deviations from (81). It has been shown – using pilot-wave field theory on de Sitter space – that if microscopic quantum nonequilibrium exists at the onset of inflation then instead of relaxing it will be preserved during the inflationary phase and then transferred to macroscopic lengthscales by the spatial expansion [18, 20].

For each mode, the width of the evolving nonequilibrium distribution maintains a constant ratio with the width of the equilibrium distribution. This was

⁵Note that (80) becomes singular if one literally takes the slow-roll limit $\dot{\phi}_0 \rightarrow 0$. The formula should be understood to be valid in the near-de Sitter regime and not for a strict de Sitter expansion. This simple treatment suffices for our purposes.

shown by calculating the de Broglie-Bohm trajectories for the inflaton field. Again writing $\phi_{\mathbf{k}}$ in terms of the real quantities $q_{\mathbf{k}r}$ ($r = 1, 2$), the Bunch-Davies wave functional takes a product form $\Psi[q_{\mathbf{k}r}, t] = \prod_{\mathbf{k}r} \psi_{\mathbf{k}r}(q_{\mathbf{k}r}, t)$ where $|\psi_{\mathbf{k}r}|^2$ is a contracting Gaussian packet of width

$$\Delta_k(\eta) = \Delta_k(0) \sqrt{1 + k^2 \eta^2}$$

(where $\eta = -1/Ha$ is conformal time, running from $-\infty$ to 0). In the late-time limit $|\psi_{\mathbf{k}r}|^2$ approaches a static Gaussian of width $\Delta_k(0) = H/\sqrt{2k^3}$. Using the de Broglie equation of motion (9) it was found that the trajectories take the form

$$q_{\mathbf{k}r}(\eta) = q_{\mathbf{k}r}(0) \sqrt{1 + k^2 \eta^2}.$$

From this result one may construct the time evolution of an arbitrary nonequilibrium distribution $\rho_{\mathbf{k}r}(q_{\mathbf{k}r}, \eta)$. It is readily seen that $\rho_{\mathbf{k}r}$ is a contracting distribution of width

$$D_{\mathbf{k}r}(\eta) = D_{\mathbf{k}r}(0) \sqrt{1 + k^2 \eta^2}$$

(with arbitrary $D_{\mathbf{k}r}(0)$). In the late-time limit $\rho_{\mathbf{k}r}$ approaches a static packet of width $D_{\mathbf{k}r}(0)$. The overall time evolution amounts to a homogeneous contraction of both $\rho_{\mathbf{k}r}$ and $|\psi_{\mathbf{k}r}|^2$ by the same factor. Thus, indeed, for each mode the widths of the nonequilibrium and equilibrium distributions remain in a fixed ratio over time [18, 20].

For simplicity we assume that $D_{\mathbf{k}r}(t) = D_k(t)$. We may then write

$$\frac{D_k(t)}{\Delta_k(t)} = (\text{const. in time}) \equiv \sqrt{\xi(k)}. \quad (84)$$

We then have a nonequilibrium variance

$$\langle |\phi_{\mathbf{k}}|^2 \rangle = \langle |\phi_{\mathbf{k}}|^2 \rangle_{\text{QT}} \xi(k), \quad (85)$$

with a ‘nonequilibrium function’ $\xi(k) \neq 1$. The nonequilibrium power spectrum for $\mathcal{R}_{\mathbf{k}}$ is then

$$\mathcal{P}_{\mathcal{R}}(k) = \mathcal{P}_{\mathcal{R}}^{\text{QT}}(k) \xi(k) \quad (86)$$

and scale invariance is generally broken. Measurements of the angular power spectrum C_l for the CMB may then be used to set experimental bounds on $\xi(k)$ [20].

To a first approximation we may assume that the quantum-theoretical spectrum is scale invariant: $\mathcal{P}_{\mathcal{R}}^{\text{QT}}(k) \approx \text{const.}$. In the low- l region we then have, from (79),

$$\frac{C_l}{C_l^{\text{QT}}} \approx 2l(l+1) \int_0^\infty \frac{dk}{k} j_l^2(2k/H_0) \xi(k), \quad (87)$$

where C_l^{QT} denotes the angular power spectrum predicted by quantum theory and C_l denotes that predicted by nonequilibrium pilot-wave theory. As was

pointed out in ref. [20], a low-power anomaly – that is, evidence for $C_l < C_l^{\text{QT}}$ – may be explained by having $\xi(k) < 1$ in a suitable region of k -space.

Note that $\xi(k) < 1$ requires that the nonequilibrium width D_k for the inflaton mode be less than the quantum equilibrium width Δ_k . It is reasonable to expect this – as opposed to $\xi(k) > 1$ – if one accepts our basic premise that quantum noise has a dynamical origin. For it then seems natural to assume initial conditions (in this case for a pre-inflationary era) with a statistical dispersion smaller than the quantum equilibrium value – so that the initial state contains less statistical noise than a regular quantum state. If we make such an assumption, then at later times (as relaxation proceeds during the pre-inflationary period) the dispersion will reach at most the equilibrium value. Thus, while a larger-than-quantum inflationary dispersion ($\xi(k) > 1$) is possible in principle, it seems more natural to have a less-than-quantum dispersion ($\xi(k) < 1$).

The integral in (87) is dominated by the scale $k \approx lH_0/2$, so a significant drop in C_l requires $\xi(k) < 1$ for k in this region. Thus we require $\xi(k) < 1$ for comoving wavelengths

$$\lambda \sim (4\pi/l)H_0^{-1} \quad (88)$$

that are comparable to the Hubble radius H_0^{-1} today.

One might consider a simple cutoff, with $\xi(k) = 0$ for $\lambda > \lambda_c = 2\pi/k_c$. The correction to C_l will be significant only if the interval $(0, k_c)$ overlaps substantially with the scale $k \approx lH_0/2$, so that λ_c cannot be much larger than $(4\pi/l)H_0^{-1}$. If instead we had $\lambda_c \gg (4\pi/l)H_0^{-1}$ the correction to C_l would not only be small – it would be unobservable (even in principle) because it would be much smaller than the cosmic variance [20].

To explain the observed power deficit in the low- l region, then, we require a dip in quantum noise – quantified by $\xi(k) < 1$ – for modes of wavelength comparable to (88). Taking $l \lesssim 40$, we require a cutoff of order

$$\lambda_c \sim H_0^{-1} . \quad (89)$$

7.3 Infra-red cutoff λ_c from a pre-inflationary era

There are likely to be many possible mechanisms for producing such a cutoff. One scenario might involve a suitable period of ‘fast rolling’ for the inflaton field [56]. Another scenario, outlined here, would involve a radiation-dominated pre-inflationary era with suppression of quantum noise at large scales.

Let us consider a radiation-dominated pre-inflationary phase starting at an initial time t_i , with a transition to an inflationary phase occurring around a time t_f . As shown in Figure 5, the transition from pre-inflation to inflation is modelled (for simplicity) as a sudden jump at time t_f . It will be necessary to assume that H^{-1} increases across the jump, from $H_-^{-1}(t_f)$ to $H_+^{-1}(t_f) > H_-^{-1}(t_f)$.

Let us denote the approximately constant Hubble radius during inflation by H_{inf}^{-1} (equal to $H_+^{-1}(t_f)$). Relevant cosmological fluctuations – those that make a measurable contribution to the CMB – originate from inside H_{inf}^{-1} . If

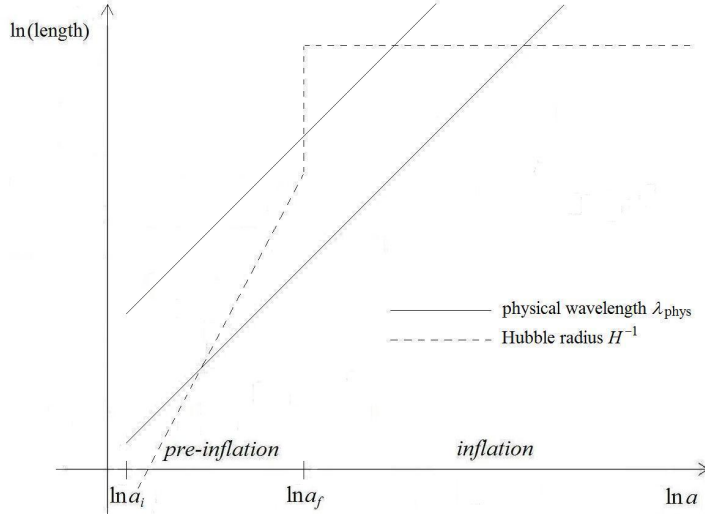


Figure 5: Inflation with a radiation-dominated pre-inflationary era. The dashed line shows the Hubble radius H^{-1} . The solid lines show physical wavelength λ_{phys} for two different modes: the lower line enters the Hubble radius during pre-inflation and exits during inflation, while the upper line remains outside the Hubble radius throughout the pre-inflationary era and enters only during the transition.

some of those modes were out of equilibrium during inflation, they must have evolved from modes that did not completely relax during the pre-inflationary phase (where the pre-inflationary modes are understood to refer to the relevant fields that were then present). Given our results for relaxation on expanding space with $a \propto t^{1/2}$, relic nonequilibrium at the end of pre-inflation is most likely to exist for modes that remained in the super-Hubble regime.

We therefore focus our attention on field modes that enter the Hubble radius during the transition from pre-inflation to inflation. As shown in Figure 5, for such modes no time is spent in the (pre-inflationary) sub-Hubble regime and therefore relaxation is likely to be suppressed. However, relaxation could still occur during the transition itself, around the time t_f . If we assume that nonequilibrium can survive the transition, then these modes can still be out of equilibrium at the beginning of inflation and make a nonequilibrium contribution to the CMB spectrum – provided $H_{-}^{-1}(t_f) < H_{\text{inf}}^{-1}$, so that modes outside the Hubble radius just before t_f can be inside the Hubble radius just after t_f .

Modes can enter the Hubble radius only if λ_{phys} increases more slowly than does H^{-1} – that is, only if the comoving Hubble radius $h^{-1} \equiv H^{-1}/a = 1/\dot{a}$ increases with time. This occurs for a decelerating universe ($\ddot{a} < 0$), which requires that the pressure p and energy density ρ satisfy $w \equiv p/\rho > -1/3$. If our putative nonequilibrium modes are to contribute to the CMB spectrum,

h^{-1} must increase during the transition from pre-inflation to inflation. To show that this could occur, let us consider how h^{-1} varies as a function of a . Writing

$$dh^{-1}/da = (1/\dot{a})dh^{-1}/dt = -(h^{-1})^3\ddot{a}$$

and using the Friedmann–Lemaître equations

$$\frac{\ddot{a}}{a} = -\frac{4\pi G}{3}(\rho + 3p) ,$$

$$\left(\frac{\dot{a}}{a}\right)^2 = \frac{8\pi G}{3}\rho$$

yields

$$\frac{d \ln h^{-1}}{da} = \frac{u}{a} ,$$

where the parameter

$$u \equiv \frac{1}{2}(1 + 3w)$$

varies from +1 to −1 as the equation-of-state parameter w varies from +1/3 to −1. We may then integrate across the transition, yielding

$$\frac{h_2^{-1}}{h_1^{-1}} = \exp\left(\int_{a_1}^{a_2} \frac{u}{a} da\right) \quad (90)$$

(where subscripts 1 and 2 denote values at the beginning and end of the transition respectively). We will have the desired increase, $h_2^{-1}/h_1^{-1} > 1$, if and only if

$$\int_{a_1}^{a_2} \frac{u}{a} da > 0 . \quad (91)$$

Because u/a ranges from $1/a_1$ to $-1/a_2$, where $a_2 > a_1$, it is plausible that this integral will indeed be positive (though logarithmically small) – in which case physical wavelengths will be driven inside the Hubble radius, thereby allowing the said modes to contribute to the CMB spectrum.

A proper discussion of the transition would require a detailed model, and it is quite possible that relaxation – or at least significant relaxation – will occur during the transition. On the other hand, the transition takes place from a pre-inflationary era of relaxation suppression for super-Hubble modes to an inflationary era of totally suppressed relaxation on all scales. It then seems possible that nonequilibrium modes that are outside the Hubble radius just before the transition will not completely relax during the transition. Here we shall simply assume that if nonequilibrium exists immediately prior to t_f then it will survive, at least to some degree, until the beginning of inflation itself. (A future strategy to model the transition is noted in Section 8.)

If we make that assumption, then nonequilibrium is possible for all modes such that $\lambda_{\text{phys}}(t_f) \gtrsim H^{-1}(t_f)$. We may then obtain an estimate for the cutoff

λ_c – the minimal comoving wavelength for which nonequilibrium is likely to exist – by setting

$$a_f \lambda_c \sim H_-^{-1}(t_f) . \quad (92)$$

The scale factor a_f (at the end of pre-inflation) may be written as

$$a_f = a_f/a_0 = (a_f/a_{\text{end}})(a_{\text{end}}/a_0) ,$$

where a_{end} is the scale factor at the end of inflation. The expansion that takes place during the transition from pre-inflation to inflation may presumably be neglected compared to the huge expansion that takes place during inflation itself. We may then approximately identify a_f with the scale factor a_{begin} at the beginning of inflation – in which case we have $a_f/a_{\text{end}} \simeq e^{-N}$, where N is the number of inflationary e-folds. If we similarly neglect the expansion that takes place during the transition from inflation to post-inflation, we can write $a_{\text{end}}/a_0 \simeq T_0/T_{\text{end}}$ (where T_{end} is the temperature at which inflation ends). Thus we have

$$a_f \simeq e^{-N}(T_0/T_{\text{end}}) \quad (93)$$

and so we find

$$\lambda_c \sim e^N H_-^{-1}(t_f) (T_{\text{end}}/T_0) . \quad (94)$$

Since (inserting c , and using the standard temperature clock $t \sim (1 \text{ s})(1 \text{ MeV}/k_B T)^2$ for a radiation-dominated era)

$$H_-^{-1}(t_f) = 2ct_f \sim 2c(1 \text{ s})(1 \text{ MeV}/k_B T_f)^2 \sim (10^{11} \text{ cm})(1 \text{ MeV}/k_B T_f)^2 ,$$

and using $k_B T_0 \sim 10^{-4} \text{ eV}$, we find

$$\lambda_c \sim (10^{-1} \text{ cm})e^N (T_{\text{end}}/T_f) (T_P/T_f) ,$$

where T_P is the Planck temperature. Writing $(1 \text{ cm}) \simeq H_0^{-1} e^{-65}$ (where $H_0^{-1} \simeq 10^{28} \text{ cm}$), we have an approximate formula

$$\lambda_c \sim 10^{-1} H_0^{-1} e^{(N-65)} (T_{\text{end}}/T_f) (T_P/T_f) \quad (95)$$

for the cutoff λ_c in terms of three parameters N , T_{end}/T_f and T_P/T_f .

This is of course only a rough estimate. Even so, because (95) was derived from essentially ‘kinematical’ arguments we may expect that the true expression for the cutoff will not be strongly model-dependent and that (95) will provide an indication of the order of magnitude. On the other hand, of course, the actual values of the parameters appearing in (95) will be strongly model-dependent.⁶

One may reasonably expect T_f to be of the same order of magnitude as the energy scale $H_{\text{inf}} \sim 10^{16} \text{ GeV} \sim 10^{-3} T_P$ associated with the inflationary phase. Thus we may take

$$T_P/T_f \sim 10^3 . \quad (96)$$

⁶One could also consider modes that enter the Hubble radius during pre-inflation (cf. Figure 5), but do not spend enough time in the sub-Hubble regime for them to relax completely. Consideration of these modes yields a small correction to the expression (95) for the cutoff [41].

Our estimate (95) for λ_c is then

$$\lambda_c \sim 10^2 H_0^{-1} e^{(N-65)} (T_{\text{end}}/T_f) . \quad (97)$$

We have two parameters: the number N of e-folds and the ‘reheating ratio’ T_{end}/T_f .

For inflation to solve the horizon and flatness problems, standard estimates indicate that the minimum number $N = N_{\text{min}}$ of e-folds required – from the beginning of inflation to the end of inflation – is $N_{\text{min}} \simeq 70$ (though some authors take $N_{\text{min}} \simeq 60$). See, for example, ref. [4]. (It is of course possible that the actual number N of e-folds is much larger than N_{min} . See, for example, ref. [58].)

The ratio T_{end}/T_f depends on the details of the reheating process. If the inflaton decay time is smaller than the Hubble time (evaluated at the end of inflation), the vacuum energy is expected to be rapidly converted into radiation. The predicted ‘reheating temperature’ T_{end} depends, among other things, on the inflaton decay rate. Estimates for T_{end}/T_f depend on the model, and can range from $T_{\text{end}}/T_f \sim 1$ to $T_{\text{end}}/T_f \ll 1$. (For overviews of the theory of reheating see, for example, refs. [4, 59].) One may also attempt to constrain T_{end} by means of CMB data [60, 61]. Martin and Ringeval [60] obtain lower bounds on T_{end} in the range 390 GeV – 890 TeV (depending on the inflationary model), corresponding to lower bounds on T_{end}/T_f in the range $\sim 10^{-14} - 10^{-10}$ (assuming $T_f \sim 10^{-3} T_{\text{P}}$).

For the estimate (97) to yield a λ_c of the required order of magnitude (89), we have the constraint

$$e^{(N-65)} (T_{\text{end}}/T_f) \sim 10^{-2} . \quad (98)$$

This is consistent with the allowed parameter space. For example, we could have $N \sim 65$ and $T_{\text{end}}/T_f \sim 10^{-2}$. To have much more than the minimal number of e-folds requires a very small reheating ratio. For example, if we allow T_{end}/T_f to be as small as $\sim 10^{-10}$ then N can range up to ~ 83 .

If instead $e^{(N-65)} (T_{\text{end}}/T_f) \gg 10^{-2}$ then $\lambda_c \gg H_0^{-1}$ and the angular power spectrum for low l will be unaffected. In this case the nonequilibrium (even if it exists) will be completely unobservable. There are of course models of inflation in which $N \gg 65$. For these, there would be no hope of detecting pre-inflationary nonequilibrium in the CMB. However, such models do lead to an alternative possibility: when $N \gg N_{\text{min}}$ it can happen that the Hubble radius today originated from a lengthscale which, at the beginning of inflation, was smaller than the Planck length [5, 6]. Such ‘trans-Planckian’ modes could be subject to novel gravitational effects that generate quantum nonequilibrium [49, 18], yielding an observable effect on the CMB [20]. A small value of N , therefore, makes it more likely that we could detect pre-inflationary nonequilibrium in the CMB; while a large value of N makes it more plausible that we could detect a Planck-scale production of nonequilibrium in the CMB (if such effects exist). There might be intermediate values of N such that neither effect would be visible. Only further and more detailed model building can tell us where such intermediate values may lie.

8 Conclusion

We have constructed an exactly-solvable model for the suppression of quantum noise at super-Hubble wavelengths in a radiation-dominated universe. The results broadly confirm expectations of a suppression of relaxation to quantum equilibrium for super-Hubble modes [18, 19, 20, 41]. The mechanism emerges naturally from pilot-wave dynamics on expanding space. We have also considered a cosmological scenario with a pre-inflationary phase, to illustrate how the mechanism might explain the large-scale power deficit that has recently been confirmed to exist in the CMB [43].

The statistical significance of the observed low- l power deficit is not high: it could be a random fluctuation for our single sky, as opposed to a genuine anomaly in the underlying power spectrum. A better understanding of the deficit and of its significance requires the development of physical models that (i) predict such a deficit, and (ii) make additional testable predictions. The first requirement has been met by showing that the de Broglie-Bohm pilot-wave theory contains a natural mechanism for producing a suppression of quantum noise at large scales on expanding space. The second requirement is a matter for future work – some suggestions will be made here.

Firstly, it would be of interest to study the detailed application of our mechanism for quantum noise suppression to specific cosmological models, with a view to predicting features of the nonequilibrium function $\xi(k)$ that modifies the inflationary power spectrum. In our scenario with a pre-inflationary phase, for example, one could study the evolution of nonequilibrium in the pre-inflationary era – including across the transition to inflation. This would require a model of the transition. Given the scale factor $a = a(t)$ as a function of time during the transition, it should be possible to solve the ordinary differential equations (20)–(22) (at least numerically) and thereby obtain the wave functional for the field modes. One could then calculate the de Broglie-Bohm trajectories and study how early nonequilibrium evolves across the transition. Given a prediction for $\xi(k)$, one could then make a comparison with current data – and weigh the outcome against rival explanations based on other models.

Secondly, in this paper we have focussed for definiteness on a scenario with quantum noise suppression in a radiation-dominated expansion. It is however conceivable that a pre-inflationary phase was not radiation-dominated. Our solution for the wave functional may be readily generalised to an expansion with a power law $a \propto t^p$ since, as is well known, the mode equation (25) may then be solved in terms of Bessel functions. (The phase factor Θ would still be given by the integral (33).) One could then investigate quantum noise suppression for more general spatial expansions.

Thirdly, we note that quantum nonequilibrium in the inflationary phase can generate non-Gaussianity, which can manifest as non-random phases and inter-mode correlations [20]. An early relaxation suppression could certainly generate non-Gaussian effects, though this remains to be studied in detail. While some authors have suggested that non-Gaussianity may exist in the *WMAP* data [62], little evidence for it has so far been found in the *Planck* data [63, 64].

Finally, the *Planck* team has also reported tentative evidence for anisotropy at large scales [63]. Whether or not this feature is truly primordial remains to be seen. It is in any case worth noting that a large-scale anisotropy could be generated by quantum nonequilibrium simply by allowing the width $D_{\mathbf{k}r}(t)$ of the (nonequilibrium) inflaton field distribution $\rho_{\mathbf{k}r}(q_{\mathbf{k}r}, t)$ to depend on the direction of the mode wave vector \mathbf{k} – and not just on its magnitude k as was assumed in ref. [20]. We would then have a nonequilibrium function $\xi = \xi(\mathbf{k})$ that depends on the direction of \mathbf{k} . If such a non-isotropic nonequilibrium existed in a pre-inflationary phase, isotropy would be recovered in the inflationary era for those modes that relaxed to equilibrium – since the inflationary equilibrium width $\Delta_k(t)$ depends only on $|\mathbf{k}|$ (and t). On the other hand, if relaxation suppression occurs for long-wavelength modes during pre-inflation then the anisotropy will presumably remain at large scales during inflation – along with the power deficit. We therefore seem to have a single mechanism whereby both a power deficit and a statistical anisotropy can be generated at large angular scales in the CMB. Whether such a scenario could provide a good fit to the *Planck* data is left for future analysis.

Acknowledgements. AV wishes to thank Patrick Peter for helpful discussions and comments on the manuscript. This research was funded jointly by the John Templeton Foundation and Clemson University.

References

- [1] A. R. Liddle and D. H. Lyth, *Cosmological Inflation and Large-Scale Structure* (Cambridge University Press, Cambridge, 2000).
- [2] V. Mukhanov, *Physical Foundations of Cosmology* (Cambridge University Press, Cambridge, 2005).
- [3] S. Weinberg, *Cosmology* (Oxford University Press, 2008).
- [4] P. Peter and J.-P. Uzan, *Primordial Cosmology* (Oxford University Press, 2009).
- [5] R. H. Brandenberger and J. Martin, *Mod. Phys. Lett. A* **16**, 999 (2001). [arXiv:astro-ph/0005432]
- [6] J. Martin and R. H. Brandenberger, *Phys. Rev. D* **63**, 123501 (2001). [arXiv:hep-th/0005209]
- [7] J. C. Niemeyer, *Phys. Rev. D* **63**, 123502 (2001). [arXiv:astro-ph/0005533]
- [8] J. C. Niemeyer and R. Parentani, *Phys. Rev. D* **64**, 101301 (2001). [arXiv:astro-ph/0101451]
- [9] J. Kowalski-Glikman, *Phys. Lett. B* **499**, 1 (2001). [arXiv:astro-ph/0006250]

- [10] A. Kempf, Phys. Rev. D **63**, 083514 (2001). [arXiv:astro-ph/0009209]
- [11] A. Kempf and J. C. Niemeyer, Phys. Rev. D **64**, 103501 (2001). [arXiv:astro-ph/0103225]
- [12] R. Easther, B. R. Greene, W. H. Kinney and G. Shiu, Phys. Rev. D **64**, 103502 (2001). [arXiv:hep-th/0104102]
- [13] F. Lizzi, G. Mangano, G. Miele and M. Peloso, J. High Energy Phys. **06**, 049 (2002). [arXiv:hep-th/0203099]
- [14] U. H. Danielsson, Phys. Rev. D **66**, 023511 (2002). [arXiv:hep-th/0203198]
- [15] A. Perez, H. Sahlmann and D. Sudarsky, Class. Quantum Grav. **23**, 2317 (2006). [arXiv:gr-qc/0508100]
- [16] J. Martin, V. Vennin and P. Peter, Phys. Rev. D **86**, 103524 (2012). [arXiv:1207.2086]
- [17] P. Cañate, P. Pearle and D. Sudarsky, Phys. Rev. D **87**, 104024 (2013). [arXiv:1211.3463]
- [18] A. Valentini, J. Phys. A: Math. Theor. **40**, 3285 (2007). [arXiv:hep-th/0610032]
- [19] A. Valentini, De Broglie-Bohm prediction of quantum violations for cosmological super-Hubble modes, arXiv:0804.4656 [hep-th].
- [20] A. Valentini, Phys. Rev. D **82**, 063513 (2010). [arXiv:0805.0163]
- [21] L. de Broglie, in: *Électrons et Photons: Rapports et Discussions du Cinquième Conseil de Physique* (Gauthier-Villars, Paris, 1928). [English translation in ref. [22].]
- [22] G. Bacciagaluppi and A. Valentini, *Quantum Theory at the Crossroads: Reconsidering the 1927 Solvay Conference* (Cambridge University Press, 2009). [arXiv:quant-ph/0609184]
- [23] D. Bohm, Phys. Rev. **85**, 166 (1952).
- [24] D. Bohm, Phys. Rev. **85**, 180 (1952).
- [25] P. R. Holland, *The Quantum Theory of Motion: an Account of the de Broglie-Bohm Causal Interpretation of Quantum Mechanics* (Cambridge University Press, Cambridge, 1993).
- [26] W. Struyve and A. Valentini, J. Phys. A: Math. Theor. **42**, 035301 (2009). [arXiv:0808.0290]
- [27] A. Valentini, in: *Many Worlds? Everett, Quantum Theory, and Reality*, eds. S. Saunders *et al.* (Oxford University Press, 2010). [arXiv:0811.0810]

- [28] A. Valentini, Phys. Lett. A **156**, 5 (1991a).
- [29] A. Valentini, Phys. Lett. A **158**, 1 (1991b).
- [30] A. Valentini, PhD thesis, International School for Advanced Studies, Trieste, Italy (1992). [www.sissa.it/ap/PhD/Theses/valentini.pdf]
- [31] A. Valentini, in: *Bohmian Mechanics and Quantum Theory: an Appraisal*, eds. J. T. Cushing *et al.* (Kluwer, Dordrecht, 1996).
- [32] A. Valentini, in: *Chance in Physics: Foundations and Perspectives*, eds. J. Bricmont *et al.* (Springer, Berlin, 2001). [arXiv:quant-ph/0104067]
- [33] A. Valentini, Pramana – J. Phys. **59**, 269 (2002). [arXiv:quant-ph/0203049]
- [34] A. Valentini, Physics World **22N11**, 32 (2009). [arXiv:1001.2758]
- [35] P. Pearle and A. Valentini, in: *Encyclopaedia of Mathematical Physics*, eds. J.-P. Francoise *et al.* (Elsevier, North-Holland, 2006). [arXiv:quant-ph/0506115]
- [36] A. Valentini, in: *Einstein, Relativity and Absolute Simultaneity*, eds. W. L. Craig and Q. Smith (Routledge, London, 2008). [arXiv:quant-ph/0504011]
- [37] A. Valentini and H. Westman, Proc. Roy. Soc. Lond. A **461**, 253 (2005). [arXiv:quant-ph/0403034]
- [38] C. Efthymiopoulos and G. Contopoulos, J. Phys. A: Math. Gen. **39**, 1819 (2006).
- [39] M. D. Towler, N. J. Russell, and A. Valentini, Proc. Roy. Soc. Lond. A **468**, 990 (2012). [arXiv:1103.1589]
- [40] S. Colin, Proc. Roy. Soc. Lond. A **468**, 1116 (2012). [arXiv:1108.5496]
- [41] A. Valentini, *Hidden Variables in Modern Physics and Beyond* (Cambridge University Press, forthcoming).
- [42] C. L. Bennett *et al.*, Astrophys. J. Suppl. Ser. **192**, 17 (2011). [arXiv:1001.4758]
- [43] Planck Collaboration: P. A. R. Ade *et al.*, *Planck* 2013 results. XV. CMB power spectra and likelihood, arXiv:1303.5075.
- [44] A. Vilenkin and L. H. Ford, Phys. Rev. D **26**, 1231 (1982).
- [45] A. D. Linde, Phys. Lett. B **116**, 335 (1982).
- [46] A. A. Starobinsky, Phys. Lett. B **117**, 175 (1982).
- [47] B. A. Powell and W. H. Kinney, Phys. Rev. D **76**, 063512 (2007).
- [48] I.-C. Wang and K.-W. Ng, Phys. Rev. D **77**, 083501 (2008).

- [49] A. Valentini, Black holes, information loss, and hidden variables, arXiv:hep-th/0407032.
- [50] T. Padmanabhan, *Structure Formation in the Universe* (Cambridge University Press, Cambridge, 1993).
- [51] J.-Y. Ji, J. K. Kim, S. P. Kim and K.-S. Soh, Physical Review A **52**, 3352 (1995).
- [52] H. R. Lewis, Phys. Rev. Lett. **18**, 510 (1967).
- [53] H. R. Lewis and W. B. Riesenfeld, J. Math. Phys. **10**, 1458 (1969).
- [54] I. S. Gradshteyn and I. M. Ryzhik, *Table of Integrals, Series and Products*, seventh edition, eds. A. Jeffrey and D. Zwillinger (Academic Press, Elsevier, 2007).
- [55] E. Abraham and A. Valentini, in preparation.
- [56] C. R. Contaldi, M. Peloso, L. Kofman, and A. Linde, J. Cosm. Astropart. Phys. **07**, 002 (2003). [arXiv:astro-ph/0303636]
- [57] D. H. Lyth and A. Riotto, Phys. Rep. **314**, 1 (1999). [arXiv:hep-ph/9807278]
- [58] J. Martin, Inflationary cosmological perturbations of quantum-mechanical origin, arXiv:hep-th/0406011.
- [59] R. Allahverdi, R. Brandenberger, F.-Y. Cyr-Racine and A. Mazumdar, Annu. Rev. Nucl. Part. Sci. **60**, 27 (2010). [arXiv:1001.2600]
- [60] J. Martin and C. Ringeval, Phys. Rev. D **82**, 023511 (2010). [arXiv:1004.5525]
- [61] J. Mielczarek, Phys. Rev. D **83**, 023502 (2011). [arXiv:1009.2359]
- [62] A. P. S. Yadav and B. D. Wandelt, Phys. Rev. Lett. **100**, 181301 (2008). [arXiv:0712.1148]
- [63] Planck Collaboration: P. A. R. Ade *et al.*, *Planck* 2013 results. XXIII. Isotropy and statistics of the CMB, arXiv:1303.5083.
- [64] Planck Collaboration: P. A. R. Ade *et al.*, *Planck* 2013 results. XXIV. Constraints on primordial non-Gaussianity, arXiv:1303.5084.